INVESTIGATION OF THE DIFFERENCE IN COOL FLAME CHARACTERISTICS BETWEEN PETROLEUM DIESEL AND SOYBEAN BIODIESEL OPERATING IN LOW TEMPERATURE COMBUSTION MODE

A Thesis

by

ADITYA MUTHU NARAYANAN

Submitted to the Office of Graduate and Professional Studies
Texas A&M University
in partial fulfillment of the requirement for the degree of

MASTER OF SCIENCE

Chair of Committee,	Timothy Jacobs
Committee Members,	Jerald Caton
	Jorge Alvarado
Head of the Department,	Andreas Polycarpou

December 2013

Major Subject: Mechanical Engineering

ABSTRACT

One of the promising solutions to rising emission standards is the in-cylinder emission reduction, through low temperature combustion. Low temperature combustion defeats conventional soot-NO_x trade off by simultaneous reduction of both emissions by controlling the in-cylinder temperature below the Soot and NO_x forming temperature zones.

The use of low temperature combustion strategy phases the combustion into the expansion stroke, making the entire combustion process highly sensitive to start of high temperature combustion. Early start of high temperature combustion results in the advancement of combustion, resulting in higher in-cylinder temperature and pressure promoting the formation of oxides of nitrogen. Delayed start of combustion results in the retardation of the high temperature combustion further into the expansion stroke the first stage combustion, in this case cool flame combustion, has an important role to play in the phasing of high temperature combustion, associated emissions and efficiency.

The focus of this study is to investigate the difference in the cool flame combustion characteristics between petroleum diesel and soybean biodiesel, when operating in low temperature combustion mode. Previous studies have attributed the absence of the cool flame in biodiesel purely due to oxygen content of the biodiesel. Cycle-to-cycle variation, exhaust gas constituents, rail pressure and fuel penetration length were

analyzed to determine the causes for difference in the cool flame characteristic between the two fuels. The result of the analysis was that cool flame combustion is present in all combustion processes and not a product of systematic error or due to the combustion of the partially combusted species in the recirculated exhaust gas. It does not entirely depend on the chemical composition of fuel and rather on the in-cylinder conditions in particular the ambient oxygen concentration. Lower ambient oxygen concentration causes the cool flame to advance with respect to the high temperature heat release, making it visible in the heat release profile. The appearance of the cool flame at increased rail pressure in biodiesel does not cause a change in the trend of ignition delay, unburned hydrocarbon or carbon monoxide with respect to rail pressure. It only results in the retardation of high temperature combustion, further into the expansion stroke.

DEDICATION

To my parents, grandparents, uncles, aunts, cousins and friends who have stood by my side supporting, encouraging me and praying for success in all my endeavors.

ACKNOWLEDGEMENTS

I would like to take this opportunity to thank all my family and friends, whose support and encouragement has made this possible. I would like to thank all my lab mates in particular Joshua Bittle for going out of the way to help me. I would also thank my great advisor Dr. Jacobs for all the encouragement and support that he has provided over the past two years and my committee members Dr. Caton and Dr. Alvarado.

The author would also like to thank TEXAS A&M UNIVERSITY for providing me this opportunity.

NOMENCLATURE

ATDC	Degrees after top dead center
BMEP	Brake mean effective pressure
CO	Carbon monoxide
EGR	Exhaust gas recirculation
HC	Hydrocarbon(s)
NO	Nitric oxide
NOx	Nitrogen oxides
PM	Particulate matter
η_{eff}	Combustion efficiency
LTC	Low temperature combustion

TABLE OF CONTENTS

LIST OF FIGURES

Page

LIST OF TABLES

Page

I. INTRODUCTION

1.1 Motivation

The thought associated with exhaust gas emissions is the carbon dioxide emissions and the associated greenhouse effect. Carbon dioxide is an emission that is a bi-product of complete combustion, which can be only curtailed by the quantity of fuel combusted [1]. There are other species present in the exhaust gas, which take a toll on human health and degrade the environment, in particular the oxides of nitrogen (NO_x) and particulate matter (PM). Oxides of nitrogen is the general term given to combination NO (Nitric Oxide) and NO_2 (nitrogen-di-oxide) [2]. Nitric oxide reacts with atmospheric oxygen forming a single oxygen atom. The single oxygen atom further combines with atmospheric oxygen forming ozone, which is capable causing lung irritation and reduce respiratory system resistance to diseases. From an environmental point of view, they are capable of causing acid rains and eutrophication of coastal waters [3].

Particulate matter (PM) formed as the result on in-cylinder soot formation, has the capacity to cause various ill effects on human health based on age. In general they have the ability to cause premature death, aggravate asthma, bronchitis and decreased lung function. Environmental effects range from visibility reduction (<70%), soiling and damage of material [4].

The regulations for exhaust emission concentrations have been present from the early 1950's. These regulations limit the quantity of exhaust emissions other than carbon dioxide, which is a byproduct of complete combustion. The emission standards became more stringent from the early nineties with the introduction of Euro1 and EPA (Environmental protection agency) Tier 1 regulation, with increased global awareness of effects of the exhaust gas emissions. Ever since the standards are on the rise to which the after treatment systems have responded well, with the use ever improving filters and catalytic converters. From the introduction of the EURO1 standard in 1992 to the EURO5 standard in 2009, exhaust emission concentration of NO_x, unburned hydrocarbon and particulate emissions are reduced by 64%, 76% and 96% respectively for light duty diesel engine operations [5]. The EURO 6 [6] standard set to be introduced late in 2014 is set to reduce the emission concentration even further for NO_x and unburned hydrocarbon emissions, reducing its acceptable emission concentration by 84% and 82% in comparison to EURO 1 standard. A similar scenario exists in the EPA standards [7]. Table 1 and Table 2 [8] represented below show the various EPA and EURO standard along with acceptable emission species concentration for diesel engine combustion.

Table 1: EURO emission standards for light duty diesel engines (ppm)

Tier	*Date*	*CO*	*THC*	*NMHC*	*NOx*	*HC+ NO_x*	*PM*
Euro 1	Jul-92	2.72	-	-	-	0.97	0.14
Euro 2	Jan-96	1	-	-	-	0.7	0.08
Euro 3	Jan-00	0.64	-	-	0.5	0.56	0.05
Euro 4	Jan-05	0.5	-	-	0.25	0.3	0.025
Euro 5	Sep-09	0.5	-	-	0.18	0.23	0.005
Euro 6	Sep-14	0.5	-	-	0.08	0.17	0.005

Table 2: Emission standards in the USA for light duty diesel engines (ppm)

Year	Reference	CO	HC	HC + NOx	PM
1992	-	17.3-32.6	2.7-3.7	-	-
1996	-	5.0-9.0	-	2.0-4.0	-
2000	EPA Tier 1	2.72-6.90	-	0.97-1.70	0.14-0.25
2005	EPA Tier 2	1.0-1.5	-	0.7-1.2	0.08-0.17

The large-scale reduction of exhaust emission concentrations increases the pressure on the after treatments systems. In order to meet the future emission requirements with current after treatment system technologies, increase in size of the after treatment system is required accompanied by reduction in fuel conversion efficiency. Given the negative impact of both NO_x and PM to the environment and human health [3,4], their simultaneous reduction is required. Conventional combustion mode does not permit this due to the existence of an inverse relationship between NO_x and PM, when operating in this mode [9]. The simultaneous reduction can be obtained with use of low temperature combustion strategy. Among the exhaust gas species NO_x is most difficult to treat in the after treatment systems. The use of the low temperature combustion system will aid in the decrease of the complexity of the after treatment system that used.

One low temperature combustion strategy phases the combustion into the expansion stroke, making the entire combustion process highly sensitive to start of high temperature combustion. Early start of high temperature combustion results in the advancement of combustion, resulting in higher in-cylinder temperature and pressure promoting the formation of oxides of nitrogen [10]. Delayed start of combustion results in the retardation of the high temperature combustion further into the expansion stroke, increasing the concentration of unburned hydrocarbon in the exhaust. This is due to the decrease in local temperature to allow complete oxidation of the fuel [11]. Hence the first stage combustion, in this case cool flame combustion has an important role to play in the phasing of high temperature combustion, associated emissions and efficiency. The

distinguishing factors of high temperature combustion from cool flame combustion are the difference in is the peak heat release rates and the temperature profile (NTC temperature profile for cool flame combustion).

Previous studies have shown a strong influence of the first stage combustion on the second stage high temperature combustion processes, when operating under low temperature combustion mode [12] . The works of Tompkins et al. [13] has shown a difference in the fist stage combustion (cool flame) between conventional petroleum diesel and biodiesel. The characteristic target of this thesis study is the difference in the cool flame combustion between the two fuels. The concepts of low temperature combustion, cool flame reaction will be explained in the following sections. This will be followed by a detailed explanation of the experimental setup and methodology, results and conclusions.

1.2 Background

1.2.1 Cool flame

Flames having temperature lower than 400 ^{0}C [14] and lower reaction vigor, release of lower heat, light and carbon-di-oxide in comparison to conventional flame are termed as cool flames. The cool flame spectrum is dominated by blue and violet, and has an overall pale blue color [15].

Cool flame was first discovered Sir Humphry Davy in 1810. The properties that made him notice the cool flame was incapability to burn his fingers and ignite matches. In addition he also noticed that cool flame had the capability to change to conventional flame at certain chemical compositions and temperatures with out the aid of an external combustion source [16]. Harry Julius Emeléus, who called it cold flame, was the first to make a spectral observation of cool flame [17].

The study of cool flame gained importance in the field of internal combustion engines due to the fact that it was the source engine knock [16] for engines utilizing low octane fuel. The concomitant increase of temperature and pressure upstream of the spark plug could produce a cool flame. The cool flame has the capability of igniting a second flame front, before the arrival of the primary one. The collision of the flame fronts produces an undesirable, erratic noisy combustion termed as engine knock. This engine knock can have deteriorating effect on the life of the engine life[18] [19].

The mechanism by which cool flame is formed can be classified into four stages [20], initiation, propagation, termination and branching. The overall mechanism involved is very complex and simplified version of the mechanism presented in literature [20] is presented in the section. The first stage is the abstraction reaction with high activation energy. The reaction is selective and slow in nature. The high activation energy is provided by the collision of the oxygen atoms with the fuel molecules. The reaction

involves the removal of the hydrogen atom from the fuel forming a radical with one open site and hydroperoxide. This is indicated in Reaction 1.

$$RH + O_2 \rightarrow R^* + HO_2^* \text{.....(1)}$$

The fuel radical is capable of undergoing two chemical reactions depending on the temperature. The two reactions presented below represent both of possible outcomes.

$$R^* + O_2 \leftrightarrow RO_2^* \text{.....(2)}$$

$$R^* + O_2 \rightarrow Alkene + HO_2^* \text{ .....(3)}$$

The reaction presented in Equation 2 is highly stable at lower temperatures. A simple collision will break the reaction product back to its original constituents. Due to the low energy required reaction proceeds in the forward direction. This reaction is mainly responsible for the cool flame associated with combustion. The forward and reverse reaction attain an equilibrium, where in the temperature is maintained constant or has a negative temperature coefficient (NTC) [21]due to the fact of absorbing heat from the environment for the forward reaction.

At higher temperatures the collision of RO^*_2 results in the reaction to proceed according to Reaction 3. This causes high temperature sensitivity of cool flame.

During the engine operation, the temperature and pressure increase in the cylinder to transform the cool flame to high temperature combustion limiting the number cool flames to one. Unlike the spark ignition engines the cool flame does not have deteriorating effect in diesel engine combustion. Instead it may cause a change in the combustion phasing of the high temperature combustion. This makes the study of the cool flame important given the sensitivity of LTC to combustion phasing.

1.2.2 Low temperature combustion

Gasoline engines have become progressively cleaner in operation mostly with the use of advanced catalytic converters [22], which are more difficult to implement for the control of diesel engine emissions. This requires diesel engines to have more complex after treatment systems. Another method for the control of diesel engines is to reduce the in-cylinder formation. Low temperature combustion provides a method for doing this. Low temperature combustion can be achieved in several ways; one method that is utilized in this study is to utilize EGR and late injection timing to obtain lower emissions in comparison to conventional combustion.

Low temperature combustion is mostly known for the simultaneous reduction of soot and NO_x, which is difficult to accomplish with conventional combustion due to the inverse relationship existing between the two. The late injection timing, near top dead center results in the combustion reaction occurring late in the expansion stroke. During

the expansion stroke the pressure of the cylinder contents is reduced, due to the movement of the piston away from the top dead center. In addition to this the high EGR level results in further reduction of the overall combustion temperature and pressure. EGR acts as a diluent, undergoing sensible heating by absorbing energy from the combustion of the fuel, reducing combustion temperature. The reduction in temperature prevents the pyrolysis of fuel at fuel rich centers, reducing soot. In addition to this the reduction in temperature prevents the oxidation of nitrogen. Further the EGR increases the ignition delay by increasing the combustible mixture formation duration, further phasing the combustion into the expansion stroke.

Like many other advanced combustion strategies LTC is associated with higher CO (carbon monoxide) and HC (unburned hydrocarbon) emissions. This is partially due to the phasing of the combustion process into the expansion stroke. As the combustion occurs in the expansion stroke, the time required for combustible mixture formation increases along with decrease in-cylinder pressure, resulting in the increase in partially combusted exhaust gas species. Even with these drawbacks, the commitment to LTC research is strong due to its advantage of simultaneous NO_x and soot reductions.

In general the attainment of LTC combustion is marked by the simultaneous reduction of soot and NO_x concentration below their concentrations in conventional combustion mode. Control strategies are being developed to attain LTC without the use of emission

measurement, for application in commercial engines. However for this study the LTC attainment will be determined via exhaust emission measurement.

Low temperature combustion is more sensitive to combustion phasing in comparison to high temperature combustion, due to the fact that minor phasing change causes the overall combustion process to be advanced/retarded with respect to the expansion stroke. The phasing with respect to the expansion stroke changes the overall emission characteristics, by changes in the peak temperature and pressure. Hence the study of the causes and effects for the presence of the cool flame prior to high temperature heat release at certain in-cylinder conditions is required for better utilization of low temperature combustion for emission reduction.

II. OBJECTIVE

Previous studies of Tompkins et al. [13] have shown the difference in cool flame combustion characteristics between low temperature combustion of biodiesel and petroleum diesel; because of the difference in cool flame characteristics, biodiesel LTC of that study showed higher fuel conversion efficiency. Tompkins had associated the absence of the cool flame of biodiesel with chemical composition of fuel, in particular the oxygen content of the fuel.

The objective of this study is to determine if the difference in the cool flame characteristics depends on the oxygen content of the fuel and if not identification of probable causes for the difference in the spatial location of cool flame between petroleum diesel and biodiesel (B100). To satisfy this objective, a different biodiesel fuel (soybean-based biodiesel) than that used by Tompkins (palm-based biodiesel) will be studied under LTC conditions and compared against petroleum diesel LTC. The studied biodiesel has the same oxygen content as palm biodiesel, but different fuel composition (as quantified by differences in cetane number).

III. EXPERIMENTAL SETUP AND METHODOLOGY

3.1 Engine and dynamometer

This thesis study was performed on a 4.5 L medium duty diesel engine. This study was made possible due to some of the advanced technologies of the engine, which include electronically controlled direct injection systems that are supplied by high pressure common rail fuel injection system, a cooled exhaust recirculation system and a variable geometry turbocharger. The engine specifications that are relevant to the study are presented in Table 3. The study makes use of two fuels commercially available: #2 petroleum diesel and soybean based biodiesel (B100), the properties of which are given in Table 4.

The medium duty test engine is coupled with an automatic feedback controlled DC dynamometer. The dynamometer is used to load the engine; an automatic feedback control holds the engine speed constant while engine load is allowed to vary as fuel energy delivery rate is held constant among all test conditions.

The low temperature combustion (LTC) condition realized in this study is made possible with the use of the custom engine controller provided by Drivven, Inc., of San Antonio, Texas, USA. Independent, individual control of all engine sub systems is made possible by the use of the engine controller, meaning the pressure maintained in the common rail

fuel injection system, the injection timing, position of the EGR valve and the quantity of fuel.

Table 3: Medium duty engine under study specifications

Engine Parameter	Value
Bore	106 mm
Stroke	127 mm
Displacement	4.5 L
Rated Power	115 kW at 2400 rev/min
Compression Ratio	16.57
Ignition	Compression
Fuel System	Electronic common rail,
	Direct injection
Air System	Exhaust gas recirculation with variable geometry turbocharger

Table 4: Summary of fuel properties of Petroleum diesel and biodiesel

Property [Standards]	Diesel #2 a	Biodiesel B100 b
Density (kg/m3) [ASTM D4052s]	825.5	885
Net heat value (MJ/kg) [ASTM D240N]	43.008	37.3
Gross heat value (MJ/kg) [ASTM D240G]	45.853	35.6
Sulfur (ppm) [ASTM D5453]	5.3	2.5
Viscosity (cSt) [ASTM D445 40C]	2.247	4.066
Cetane Number [ASTM D613]	51.3	49.6
Hydrogen (%-mass) [SAE J1829]	13.41	11.76
Carbon (%-mass) [SAE J1829]	85.81	76.95
Oxygen (%-mass) [SAE J1829]	0.78	11.29
Initial boiling point (°C) [ASTM D1160]	173.4	347
Final boiling point (°C) [ASTM D1160]	340.5	360

a- Measured or calculated by Southwest Research Institute (San Antonio, Texas)

b- Measured or calculated by the Inspectorate (Houston, Texas)

From Table 4 some important property differences between the two fuels are to be noted. The first of them is the difference in the density of the fuels. The relevance of fuel density in the study is its direct proportionality to the bulk modulus of the fuel, which could have a direct impact on the fuel injection system and the fuel injection timing. The

second is the difference in the heating values of the fuels. It is of relevance due the higher quantity of biodiesel injection required for performance comparison of the two fuels at a given operating point. The most important fuel characteristic for this study is the cetane number, which is a characteristic measure of the ignition delay of the fuel. Both fuels have comparable cetane number despite the higher oxygen content of biodiesel, which is in contrast of Tompkins study[13], which used a biodiesel with cetane number higher than 60.

3.2 Experimental test matrix

The study involves testing at two injection timings, -8^0 ATDC (after top dead center) that is termed as "conventional timing" and an injection timing 0^0 ATDC that is termed as "late timing". The duration of fuel injection was set at zero exhaust gas recirculation (EGR) and conventional injection to 2 bar BMEP (Brake mean effective pressure). Once the injection duration is set, it is maintained constant throughout the study except when changing the fuel; injection duration is modified due to difference the heating values between the two fuels.

Parameter sweeps of EGR level and fuel injection pressure (via adjustment of fuel rail pressure) at the 0^0 injection timing is performed in this study to effect varying degrees of cool flame behavior. The EGR level in the intake is varied, by changing the EGR valve position. Only one parameter is varied at a given time, rail pressure is held constant

while varying EGR and vice versa. The rail pressure is maintained at 1000 bar as EGR is varied between 10% and 36%; the maximum EGR condition of 36% is maintained during the rail pressure sweep from 600 bar to 1400 bar. Other parameters are held constant in so much as possible. Exceptions include EGR temperature, airflow rate, intake manifold pressure, and intake temperature; these parameters systematically change as EGR level.

The following Table 5 and Table 6 represent the experimental test matrix for the study. The fuels are represented by the convention of "diesel" for petroleum diesel and "bio" for biodiesel (B100). Table 5 represents the test points at conventional injection timing while Table 6 represents the test points at late injection timing. The horizontal and vertical lines in the table represent the rail pressure and EGR sweep.

Table 5: Experimental test matrix for conventional timing

EGR%/Rail Pressure	1000 bar
0%	Bio/diesel

Table 6: Experimental test matrix for late injection timing

EGR%/Rail Pressure	600 bar	800 bar	1000 bar	1200 bar	1400 bar
0%			Bio/diesel		
10%			Bio/diesel		
20%			Bio/diesel		
30%			Bio/diesel		
36%	Bio/diesel	Bio/diesel	Bio/diesel	Bio/diesel	Bio/diesel

3.3 Measurement and data acquisition

The data required for the study is obtained from several measurements namely, the in-cylinder pressure. A piezo electric transducer located through the glow plug socket is used to determine the in-cylinder pressure on crank angle resolved (0.2 degree resolution) basis. In order to remove the effect of the cycle-to-cycle variation, the data are collected for 300 consecutive cycles and analysis is performed on the 300 cycle-averaged data. In addition to this he 300 cycle-averaged data, individual cycle measurements are recorded for 50 consecutive cycles. These data will support analysis if what are perceived to be cool flame events could potentially be systematic errors introduced by every-so-often cyclic variability (e.g., an occasional very early cycle combustion event compared to more-often late cycle combustion event). In-cylinder pressure measurements are used to calculate rate of heat release, as described below.

Other measurements include carbon dioxide and carbon monoxide (non-dispersive infrared technique), exhaust manifold pressure (strain gauge transducer), exhaust manifold temperature (K type thermocouple), exhaust hydrocarbon concentration (flame ionization detection on a c3 basis), intake manifold pressure (strain gauge transducer), intake manifold temperature (K-type thermocouple), fuel mass flow rate (obtained from the fuel density and the flow rate determined using a positive displacement flow meter), engine speed (dynamometer shaft encoder), NO (chemiluminescence), smoke concentration (reflectivity technique) and brake torque (load cell). The exhaust gas samples delivered to the emission benches are heated to 190^0 C for the NO, hydrocarbon, smoke analyzers and cooled and dehumidified for the carbon dioxide and monoxide analyzers.

The uncertainty in measurement is reduced by routine calibration of the instruments. Since the general uncertainty in the measurement of engines is high due its dependence on the ambient conditions, the measurements for each test point are taken over a duration of two days and the average is used for analysis, with an uncertainty bar showing the standard deviation between the two days on which the measurements were taken.

3.4 Calculations

3.4.1 Exhaust gas recirculation

EGR level is one of the parameter sweeps performed during this study. The change in EGR level in the intake manifold is achieved by changing the position of EGR valve to the desired position. The EGR level in the intake manifold is calculated as a percentage of mass fraction of the exhaust gas in the intake. In order to do this, the CO2 concentration is measured in both the intake and exhaust flows. The exhaust species in the exhaust is limited to the ones of high concentration namely, nitrogen, oxygen, carbon di oxide, carbon monoxide and water. Some of which are directly measured (oxygen, nitrogen, CO, CO_2) and other calculated (water). Knowing the ratio of intake and exhaust CO2 concentrations enables calculation of other species in the intake, and consequently calculation of the EGR level. The species composing the EGR level are determined mostly through measurement (name, O2, CO2, and CO); others are calculated (namely, H2O and N2).

The equations that are used to calculate the exhaust gas recirculation are summarized below. They are standard equations that are used for the calculation of percentage of exhaust gas recirculation and implemented as described in Heywood [23].

By definition EGR is defined as the total mass fraction of the exhaust species present in the intake. The term 'X' in the equation below represents the mass fraction of the individual exhaust species.

$$EGR\ \% = \sum_{intake} X_{exhaust,i} \ldots\ldots(1)$$

The use of the above equation requires conversion of concentration of the exhaust gas species from molar to mass fraction. This conversion is accomplished by the following equation, where 'X' represents the mass fraction, 'Y" represents the molar fraction and 'MW represents the molecular weight.

$$X_{exhaust,i} = \frac{Y_{exhaust,i} MW_{exhaust,i}}{MW_{EGR}} \ldots\ldots.(2)$$

The water shift equilibrium reaction mechanism is used to calculate the H_2O levels. Equation 3 is a balance reaction allowing the determination of the equilibrium molar concentration of the involved species. The value of the equilibrium constant' K' is taken as 3.8 based on the recommendations in [22] for the given engine conditions. The water concentrations in the intake and the exhaust are calculated using the Equation 3.

$$Y_{H_20} = \frac{Y_{CO_2} + Y_{CO}}{1 + \frac{Y_{CO}}{K \cdot Y_{CO}} + \frac{M}{2N} \cdot (Y_{CO} + Y_{CO_2})} \ldots\ldots(3)$$

The effect of ambient carbon monoxide concentration is considered negligible in the intake water calculation. The ratio M/2N depends on the fuel type. Including the water concentration calculation coverts the dry concentration of the exhaust species to a wet basis, aiding in a more accurate mass fraction calculation.

3.4.2 Apparent heat release rate

The apparent heat release rate is calculated from the in-cylinder pressure measurements. A relatively smooth in cylinder heat release curve is obtained with a use of a digital filter to remove the high frequency noise from the raw in-cylinder pressure measurements. The heat release rate is calculated using the first law of thermodynamics, under the assumption of an ideal gas behavior and single zone combustion. The following is a summary of the heat release rate calculation method.

The following equation encompasses all the energy transfers and storage in the cylinder.

$$\frac{\delta Q_{HR}}{d\theta} - \frac{\delta W}{d\theta} - \frac{\delta Q_{HT}}{d\theta} = \frac{dU_{cv}}{d\theta} \quad \text{.....(4)}$$

where,

$\frac{\delta Q_{HR}}{d\theta} - Heat\ release\ rate\ (\frac{J}{Deg})$

$\frac{\delta W}{d\theta} - Piston\ work\ rate\ (\frac{J}{Deg})$

$\frac{dU_{cv}}{d\theta} - Internal\ energy\ change\ rate\ (\frac{J}{Deg})$

$\frac{\delta Q_{HT}}{d\theta} - Heat\ transfer\ rate\ (\frac{J}{Deg})$

The negative and positive signs in Equation 4 represent energy transfer from and to the system respectively. The equation balances all of the energy terms, satisfying the first law of thermodynamics energy conservation criteria (with the exception of mass transfer terms such as blow by or crevice flow, which are neglected in this analysis). The work term in the equation accounts for all the work done by and on the contents of the cylinder on the piston. The work is done by the system on piston during the expansion stroke and vice versa in the compression stroke. The change in internal energy term accounts for changes in the total energy stored in the cylinder contents as a function of temperature. The heat transferred from and to the surroundings is represented by the heat transfer term in the equation. In actual engines the energy addition is due to chemical mechanism of combustion occurring within the cylinder to avoid the complexities of modeling such mechanisms, heat release analysis assumes the combustion reaction adds thermal energy to the system. Due to this simplification the heat release is called as apparent heat release rate.

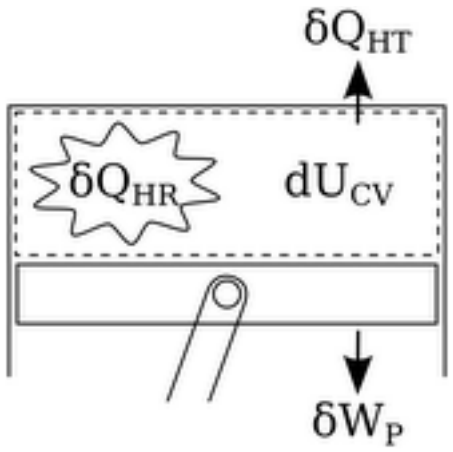

Figure 1: Energy transfer in control volume

Figure 1 is a sketch, representing the included energy transfers occurring across piston cylinder assembly. The figure is a diagrammatic representation of the equation 4. The fuel's chemical energy released during combustion is represented as thermal energy addition; hence the name apparent heat release. (Modify the corrections based on this modified language, since this paragraph will be moving to earlier in the discussion). In actual engines the heat is added by the in-cylinder combustion of fuel.

The cylinder geometry and the in-cylinder pressure measurements are used to determine the piston work term of the equation, as described by the Equation 5.

$$\frac{\delta W}{d\theta} = p \cdot \frac{dV}{d\theta} \dots\dots\dots\dots . (5)$$

where,

$p - Pressure\ (\frac{N}{m^2})$

$\frac{dV}{d\theta} -\ Rate\ of\ Volume\ change\ (\frac{m^3}{Deg})$

The gas is assumed to be ideal, making the internal energy of the cylinder contents a function of temperature. The total internal energy of the cylinder contents is a sum of the internal energy of various mixture components. The internal energy of the cylinder contents is given by the equation below.

$$dU_{CV} = \sum_{species,i} x_i m C_{v,i} \frac{dT}{d\theta} \ldots\ldots (6)$$

where,

$x_i -\ Species\ mass\ fraction$

$m -\ Total\ mass\ trapped\ in\ cylinder\ (kg)$

$C_{v,i} - Species\ specific\ heat\ at\ constant\ volume\ (\frac{J}{Kg \cdot k})$

$\frac{dT}{d\theta} - Rate\ of\ Temperature\ change\ \left(\frac{K}{Deg}\right)$

The term $C_{v,i}dT$ is used to calculate the species specific internal energy. The mass trapped in the cylinder and mass fraction of each species are to be determined individually.

The ideal gas law is used to determine the in cylinder temperature. The cylinder geometry, gas constant of the cylinder contents, mass trapped in the cylinder along with the pressure measured using the piezo-electric transducer is used to compute the temperature using the ideal gas law. The JANAF tables are used in the calculation of the species concentration and specific heat values. They are computerized tables that contain equation fits to calculate the temperature dependent species such as C_p, H, S. In addition to this the JANAF tables contain equilibrium mechanism constants that are used in the calculation of the species concentration and hence the species mass fraction. The calculation of the above parameters is used in the determination of the internal energy of the mixture at each crank angle location.

The final term in the calculation of the apparent rate of heat release is heat transfer, which is calculated using a simple model, which is represented by the Equation 6.

$$\frac{\delta Q_{HT}}{d\theta} = mAhd\left(\frac{\Delta T}{d\theta}\right) \dots\dots\dots (7)$$

where,

$\frac{\delta Q_{HT}}{d\theta} - Heat\ transfer\ rate\ (\frac{J}{Deg})$

$m - Mass\ trapped\ in\ cylinder\ (Kg)$

$h - Heat\ transfer\ Coefficient\ \left(\frac{W}{m^2 \cdot K}\right)$

$\frac{\Delta T}{d\theta} - Temperature\ Difference\ between\ cylinder\ contents\ and\ \ wall\ (\frac{K}{Deg})$

The trapped mass of the cylinder contents is known from previous calculations; the cylinder geometry is used to determine the cylinder wall area (the area perpendicular to the direction of heat transfer). The temperature difference is computed taking the difference between the temperature of the cylinder contents and cylinder wall. Since the measurements are taken at steady state condition the temperature of the cylinder wall is assumed to be constant. The equation utilized for heat transfer calculation utilizes the heat transfer coefficient developed by Hohenberg, which includes both convective and radiation heat transfer terms. This is because his model was purely convective with varied definition of characteristic length and gas reference velocity, which was consistent with most engine test results [24].

The other important parameter that is determined from the rate of heat release is the mass fraction burn (MFB) of the fuel. The heat release rate is representative of the quantity of the fuel burned. The integration of the rate of heat release quantifies the total energy released from the fuel, which divided by the total energy delivered in the entire process provides the ratio of the mass burned up to that point to the total mass burned in

the entire cycle which is termed as mass fraction burned. This parameter is useful in identifying the start of combustion (SOC).

3.4.3 Fuel penetration length

The fuel penetration length is calculated using the formula developed by Dent[25]. The fuel penetration length is determined by the formula

$$S = 3.07(\frac{\Delta p}{\rho_g})^{1/4}(td_n)^{1/2}(\frac{294}{T_g})^{1/4} \ldots\ldots (8)$$

where,

$S =$ Fuel Penetration Length (m)

$\Delta p =$ Pressure difference across fuel injector (bar)

ρ_g = Gas density at the start of injection (kg/m^3)

t = Duration of injection (seconds)

d_n= Diameter of fuel injection nozzle

T_g=Temperature of gas during injection (Kelvin)

IV. RESULTS AND DISCUSSIONS

The following section provides the necessary results and discussions to satisfy the objectives of this thesis study. For effectively achieving this, the section has been divided into five sections: 4.1) analysis of heat release rate, 4.2) effects of cycle-to-cycle variation, 4.3) effect of exhaust gas constituents 4.4) effects of rail pressure and 4.5) effects of fuel penetration and mixing. The sub-sections are organized in such a manner that the difference between the two fuels are realized, followed by analysis of various possible causes.

4.1 Analysis of heat release rate

The objective of this section is investigation of the heat release rate of petroleum diesel and biodiesel, when operating in conventional and low temperature combustion mode. An EGR sweep was studied with constant rail pressure and late injection timing to allow the direct comparison of the instantaneous heat release rates for low temperature mode of operation. An analysis of the emissions is included to confirm the low temperature operation.

Biodiesel in general is attributed with artificially advanced injection timing, due to its higher bulk modulus in comparison to petroleum diesel. Previous studies [26] [27]have shown that biodiesel has an artificial advance in injection in comparison to petroleum

diesel and that causes increased in-cylinder temperatures and pressures. This increase in temperature causes higher NO_x, lower soot and hydrocarbon emissions in comparison to petroleum diesel. The artificial advance in injection causes advance in the entire combustion process. The research by Bittle et al [28] and Tiegang Fang[29] has shown that, the case of artificial advance in injection is only true in the case of discrete injectors and not common rail injection system.

The advance in injection in biodiesel is due to the decreased time required to attain the injection pressure due to its higher incompressibility, but in the case of the common rail injection system the fuel is pressured before reaching the injector eliminating the injection timing difference between biodiesel and petroleum diesel.

Figure 2 represents the rate of heat release as a function of crank angle for conventional combustion timing of -8^0 ATDC and zero EGR averaged over 300 cycles. It can be observed from the figure that the rate of heat release of the two fuels has similar trend, magnitude and combustion phasing, despite notable differences in the physical and chemical properties from Table 4. This is due to the similarity in the cetane number between the two fuels and test point using similar energy release rate. It can also be noted that the artificial advance is not observed for biodiesel, when used in a common rail injection system. From the above it is clear that the physical properties of the fuel do not have any effect on the fuel injection system.

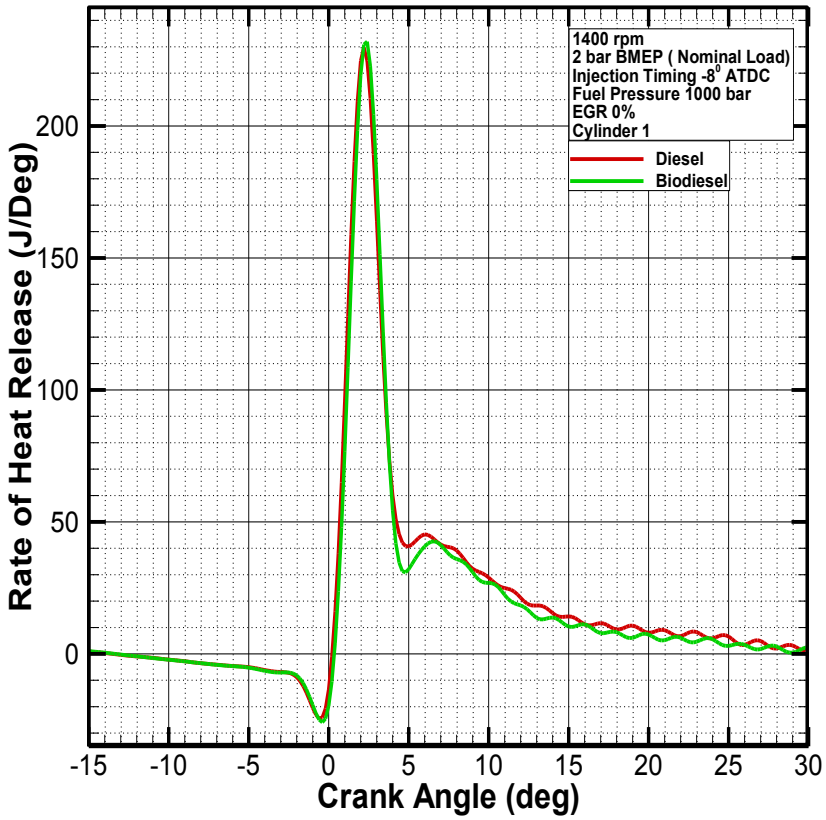

Figure 2: Rate of heat release versus crank angle for conventional combustion

Figure 3 and Figure 4 represent the instantaneous heat release rate for conventional diesel and biodiesel as a function of crank angle for various EGR conditions, which is an average of 300 cycles. A constant injection rail pressure of 1000 bar and late injection (0^0 ATDC) timing were utilized for both fuels. In Figure 3 a first "hump" is observed with a magnitude of less than 30 J/deg and in the crank angle range of 5° and 15^0. The feature exists for all EGR conditions. A similar first "hump" only starts to appear at

maximum EGR condition for biodiesel at the given rail pressure (1000 bar) represented in Figure 4.

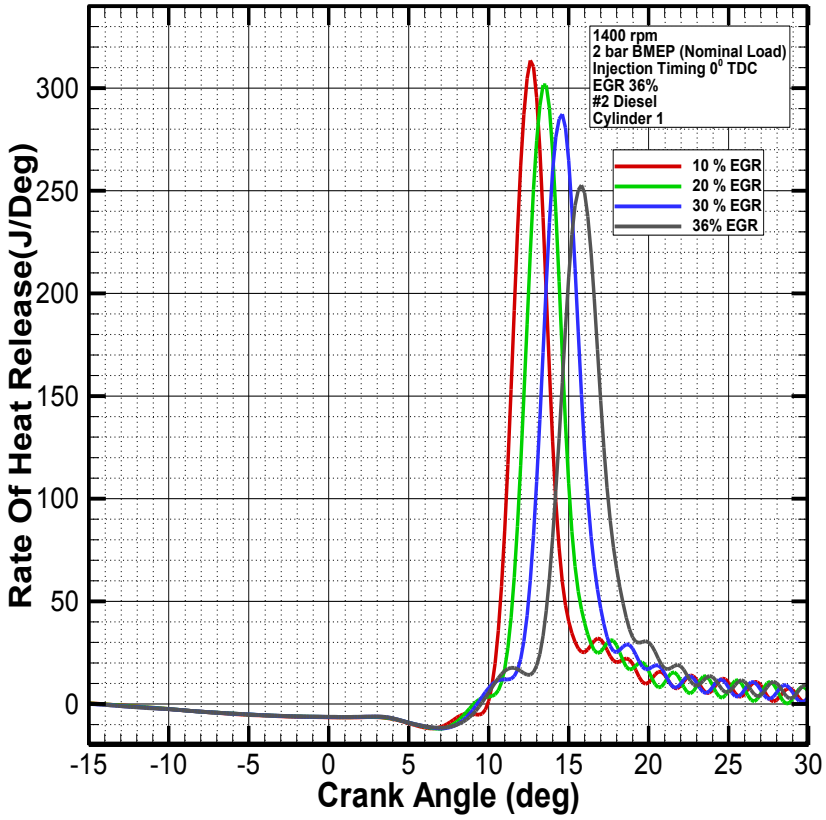

Figure 3: Rate of heat release versus crank angle for petroleum diesel operating in low temperature combustion.

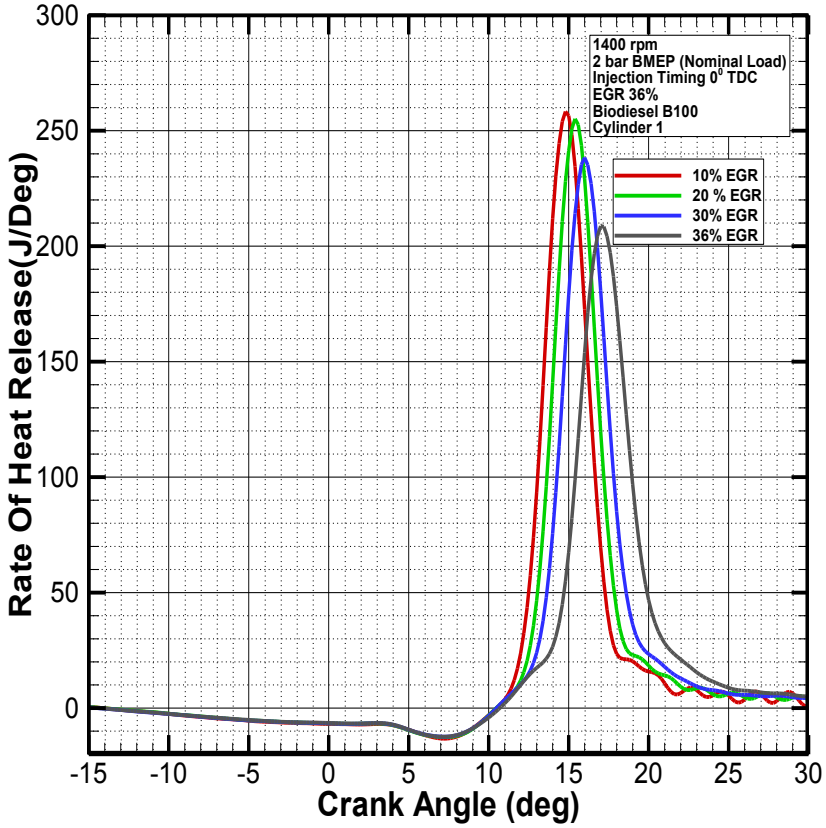

Figure 4: Rate of heat release versus crank angle for biodiesel operating in low temperature combustion mode

The next objective of the section is determination of low temperature combustion mode of operation of the test points. Low temperature combustion is used for eliminating the conventional soot-NO_x trade off and achieves the simultaneous reduction of soot and NOx. Figure 5 is a sketch of the conventional soot NO_x for any fuel operating under conventional combustion mode. It can be inferred from the sketch that decrease of one emission component causes the increase of the other. The horizontal and vertical lines

represent the minimum soot and NO_x concentrations that are achievable. For this study the relative concentration of soot is measured by the smoke meter and represented as filtered smoke number (FSN). NO concentration measured by the emissions bench is used as an indicator for the NO_x concentration.

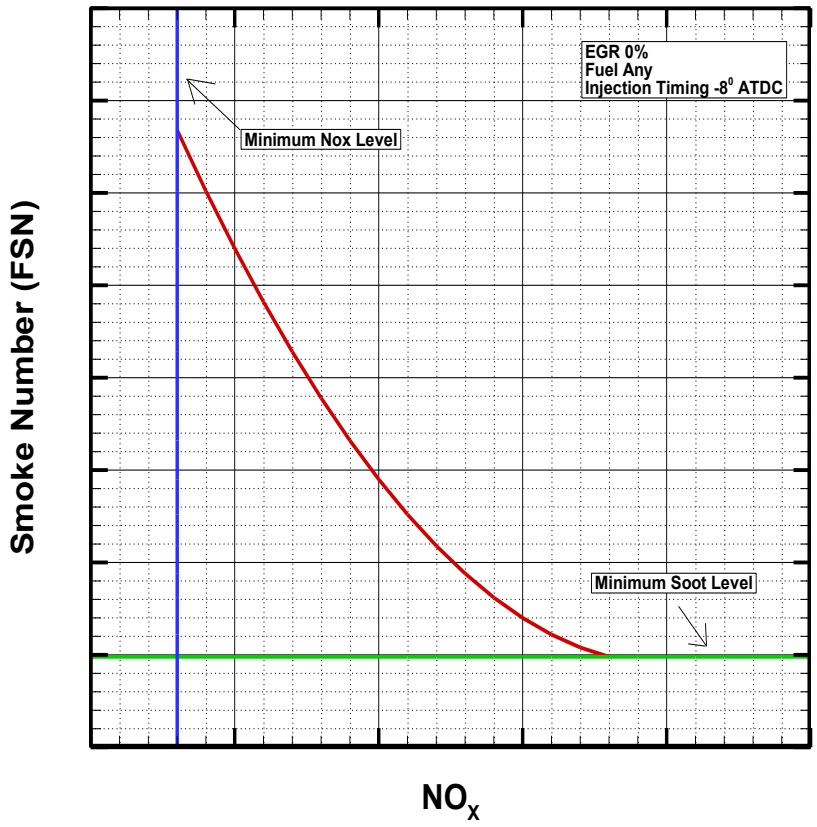

Figure 5: Traditional soot-NOx trade off for any fuel operating in conventional combustion

Figure 6 represents the soot NOx plot for petroleum diesel and biodiesel. The horizontal and vertical lines represent the soot and NOx concentration respectively at conventional injection timing and zero EGR for the given fuel, which is used as the baseline for comparison. The presence of one vertical line representing NO_x emission concentration is due to the similar NO_x emission characteristics for both fuels when operating in conventional operating mode. It can be seen from the figure that the soot and NOx concentration are lower than the baseline and the increase in soot concentration for a given decrease in NOx concentration is less than 10%. This marks the attainment of low temperature combustion.

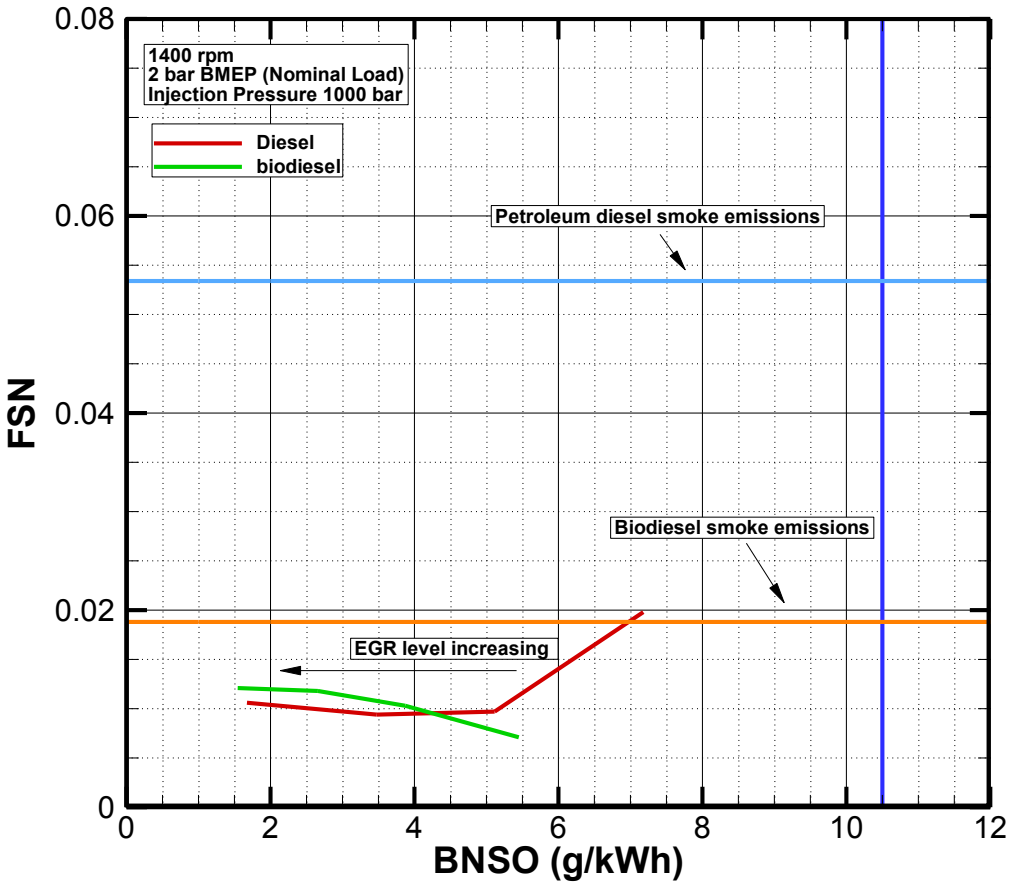

Figure 6: Soot-NO_x for low temperature combustion

In order to confirm the first hump that is observed in the case of petroleum diesel is cool flame in Figure 3, further investigation about the cool flame mechanism is required. In conventional flame combustion hydrocarbon molecules break down and react with oxygen producing carbon dioxide and water, but in the case of cool flame combustion the molecules break into larger fragments, which easily recombine with each other. A

quasi-steady equilibrium exists between the fragmentation and recombination of the fuel molecules resulting in the release of less energy and carbon dioxide in comparison to conventional flame combustion [20]. For a quasi steady equilibrium process (cool flame mechanism) there should be negative temperature coefficient (NTC) behavior[15].

Figure 7 shows the variation of rate of heat release and temperature as a function of crank angle for various EGR conditions. From the temperature profile at various EGR conditions it is evident that “hump” that is seen with petroleum diesel is indeed cool flame, as the temperature is either constant (plateau like profile) or has NTC during the cool flame duration. The end of the cool flame is indicated as a drastic change in the temperature profile.

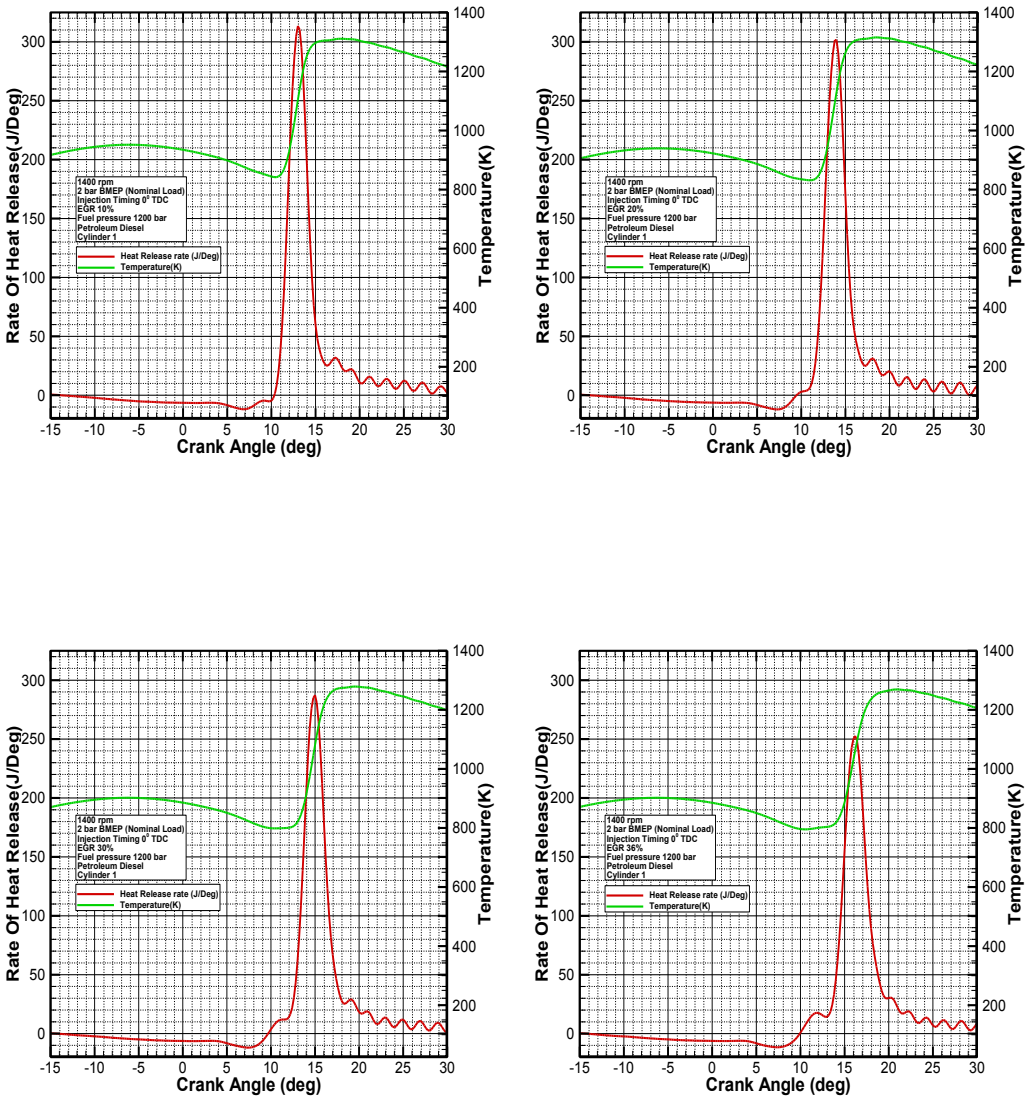

Figure 7: Rate of heat release and temperature versus crank angle for various EGR levels at 1000 bar rail pressure for petroleum diesel

Based on the optical studies conducted by Lyle et al. [30], which has demonstrated the existence of cool flame in all combustion processes a temperature profile analysis of the heat release rate of biodiesel is provided. Figure 8 shows the variation of temperature

and rate of heat release as a function of crank angle. From the Figure 4 it is evident that the cool flame does not exist at any EGR condition at the given rail pressure (1000 bar) for biodiesel. This is not contradictory to the work of Lyle et al. [30], since both the cool flame combustion and the high temperature combustion occur in the same spatial location making the cool flame undetectable in the heat release profile.

From Figure 8 it is evident that NTC condition exists before the start of high temperature combustion, which must not be directly considered as cool flame combustion. Associating the heat release profile with that of the temperature profile the NTC condition is due to the expanding volume of the piston and fuel injection and absorption of latent heat from the surroundings during the combustible mixture formation phase. This decreases the temperature of the cylinder contents before the start of high temperature combustion. However in the maximum EGR condition, a considerable heat release along with the plateau in the temperature profile is seen before the start of high temperature combustion, indicative of the upstream shift in the combustion phasing of the cool flame.

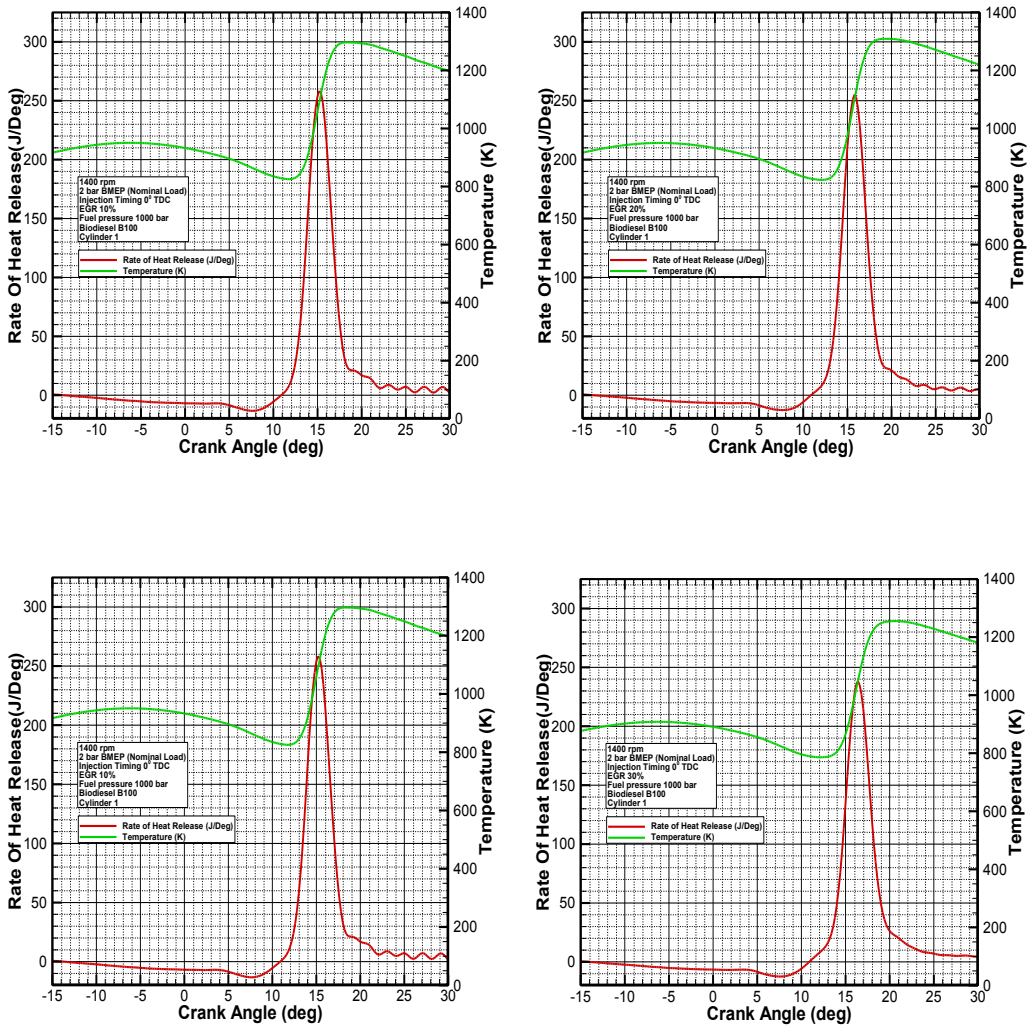

Figure 8: Rate of heat release and temperature versus crank angle for various EGR levels for biodiesel

From the above discussion it is clear that a difference in cool flame characteristics exists between petroleum diesel and biodiesel, when operating in low temperature combustion mode. In addition to this, the analysis of the heat release rate of convention combustion has revealed the negligible effect of the fuel properties on the fuel injection system, elimination as a source for the difference in the cool flame combustion characteristics. Further investigation is required to determine the causes for the difference in the cool flame characteristics. High cycle-to-cycle variation associated with diesel engines operating at low temperature combustion mode, the effect of rail pressure/injection pressure, difference in exhaust constituents between the two fuels and the effect of fuel penetration and mixture formation is analyzed in this thesis study to determine the causes of the difference in cool characteristics between the two fuels.

4.2 Effect of cycle-to-cycle variation

This section's objective is to analyze continuous cycle data to determine if systematic error is the cause for the difference in the cool flame characteristics between the two fuels. Systematic error in this case is defined as the periodic occurrence of one or more characteristics leading to a particular phenomenon. The motive for the cyclic study are the works of Knight et al[31] and Heywood [23], the former which has shown the greater sensitivity of low temperature combustion to combustion phasing in comparison to conventional combustion The fuel's chemical energy released during combustion is represented as thermal energy addition; hence the name apparent heat release. (Modify

the corrections based on this modified language, since this paragraph will be moving to earlier in the discussion). The sections objective is based on the hypothesis that the variation of one cycle could cause the combustion phasing of the subsequent cycles, due to EGR. The cycle-to-cycle variations are analyzed for 50 continuous cycles of all four cylinders to determine the existence of a pattern (systematic error) that could cause the difference of the cool flame combustion characteristics between petroleum diesel and biodiesel.

A summary of typical causes of cycle-to-cycle variation is provided as a means to guide analysis and discussion of this study's data. The cycle-to-cycle variation studies have been previously used to determine the effect of various parameters on engine performance characteristics. Yasuo Moriyoshi et al. [32] used cycle to cycle variation of in cylinder air flow in a motored engine to model external flow, extended the model to the in cylinder flow showing that swirl present within the cylinder suppresses the effect of cyclic variation. M. Zheng et al. [33] worked on the effect on non-air mixtures on cycle to cycle variation of in-cylinder pressure and temperature and determined that CO_2 was one of the major sources of variation. Maurya et al. [34] have conducted studies on cycle-to-cycle variation in combustion and emission characteristics of HCCI engines. Additional examples are provided in[35–38]. In this study, the cycle-to-cycle variation analysis is curtailed to the effect of in-cylinder combustion characteristics as a source of periodic cyclic variation in subsequent cycles. The cyclic variation analysis is

not extended to emissions due to practical limitations of the measuring capacity of the exhaust bench.

According to Heywood [23] the causes for cycle to cycle variation are gas motion (in-cylinder swirl and turbulence), amount of fuel injected, air, EGR and variations in mixture composition. The variations of gas motion and air intake are independent of the fuel injected, and the studies of Yasuo Moriyoshi et al. [32] have shown that the variations of the two counteract each other, reducing variation.. The variation in the in-cylinder mixture formation is beyond the scope of this study, leaving behind the effect of EGR for analysis. EGR has a complex effect on in-cylinder combustion process. Previous studies on the effect of EGR on diesel combustion have revealed that EGR causes a change in the ignition delay, which directly controls the combustion phasing. Given the sensitivity of low temperature combustion to combustion phasing the cyclic variation of combustion phasing is analyzed by studying cycle-to-cycle variation of 50 % mass fraction burn location and location of maximum heat release rate and ignition delay. In addition to this overall combustion variation is analyzed by the use of IMEP (indicated mean effective pressure).

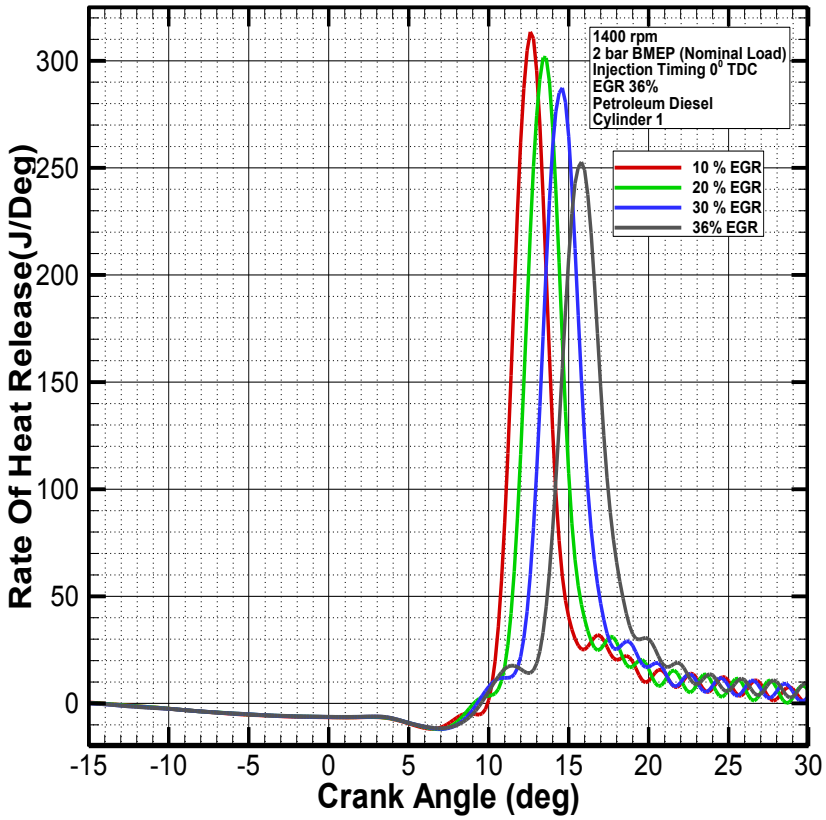

Figure 9: Rate of heat release versus crank angle as a function of EGR for petroleum diesel

The heat release profiles presented in section 4.1 are averaged over 300 continuous cycles. Figure 9 and Figure 10 represents heat release rate as a function of crank angle for various EGR levels, which are averaged over 50 cycles. The variation of combustion characteristics of the same 50 cycles is used to determine the effect of systematic error on cool flame combustion. From the figures it is evident that the difference in cool flame characteristics exists irrespective of the number of averaged cycles.

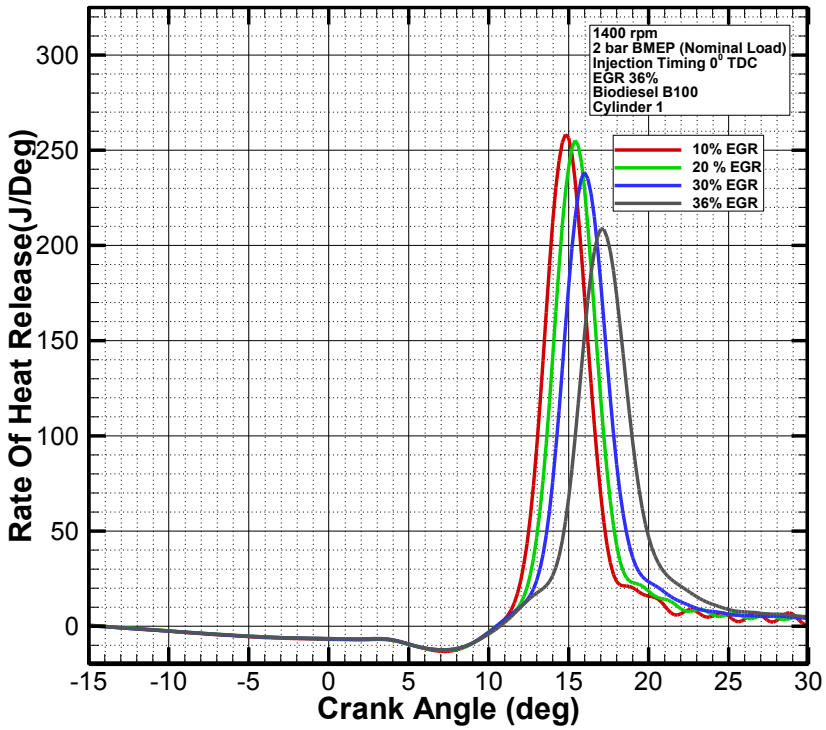

Figure 10: Rate of heat release versus crank angle as a function of EGR for biodiesel

Figure 11 to Figure 16 represents the cyclic variation of location of peak pressure, maximum heat release rate and location of 50% mass fraction burn respectively for conventional petroleum diesel. The data are represented for cylinder 1, which is representative of all four cylinders. Each combustion characteristic is analyzed for all EGR levels are studied.

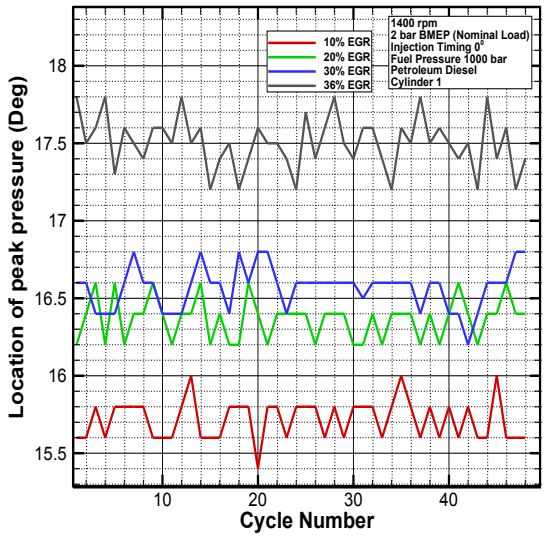

Figure 11: Location of peak pressure versus crank angle for petroleum diesel

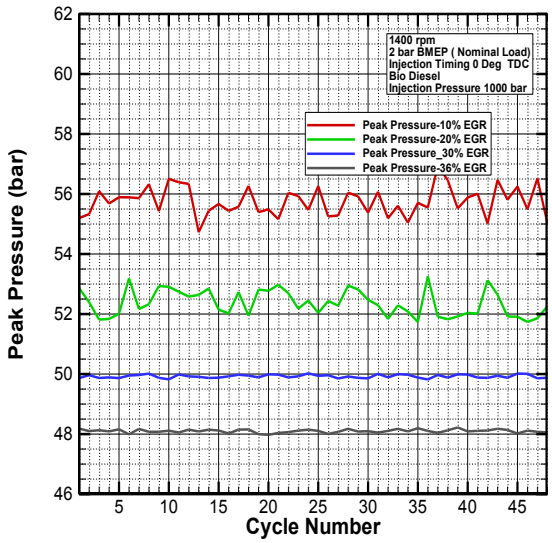

Figure 12: Peak pressure versus crank angle for petroleum diesel

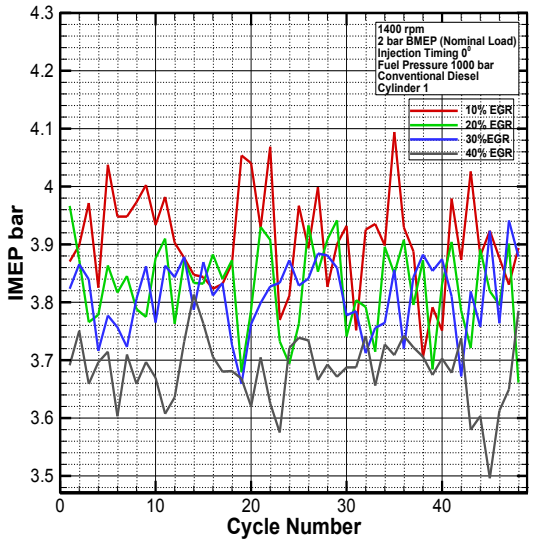

Figure 13: IMEP versus crank angle for petroleum diesel

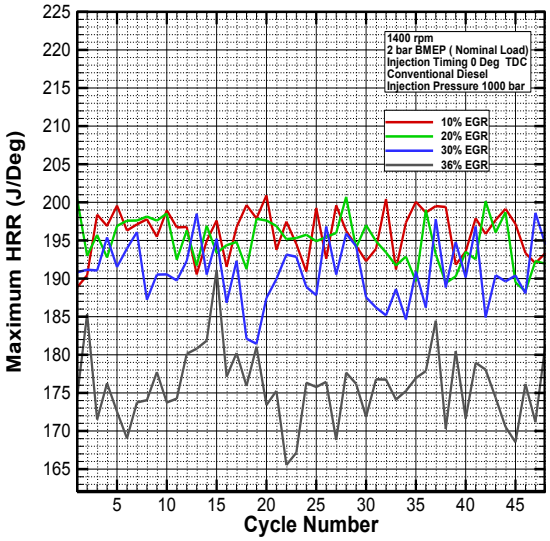

Figure 14: Maximum heat release rate versus cycle number for petroleum diesel

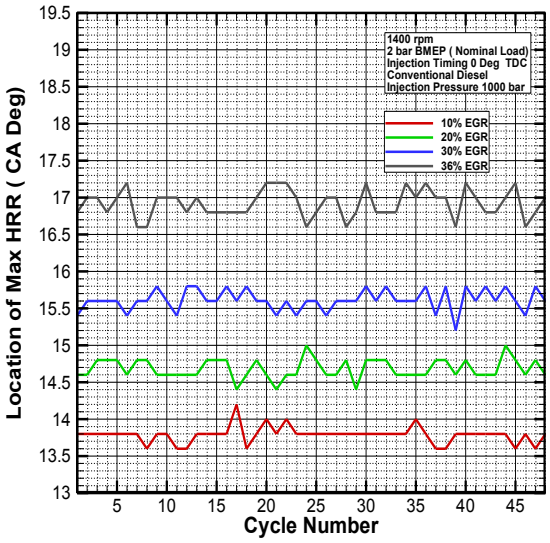

Figure 15: Location of maximum heat release rate versus cycle number for petroleum diesel

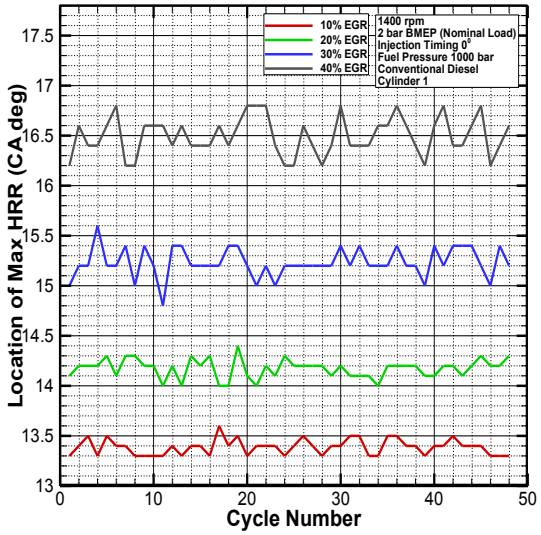

Figure 16: Location for maximum heat release rate versus cycle number for conventional diesel

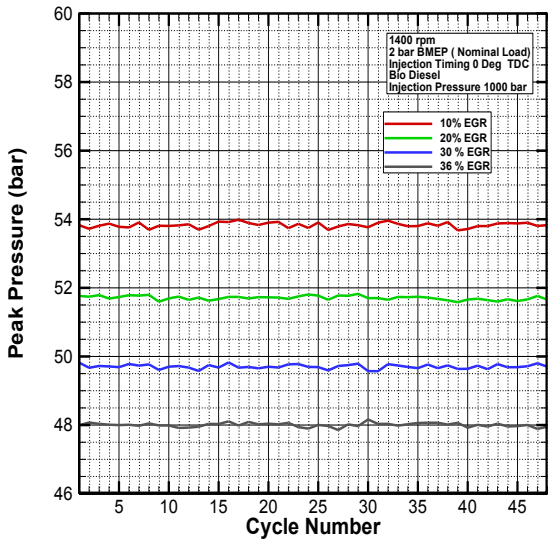

Figure 17: Peak Pressure versus cycle number for biodiesel

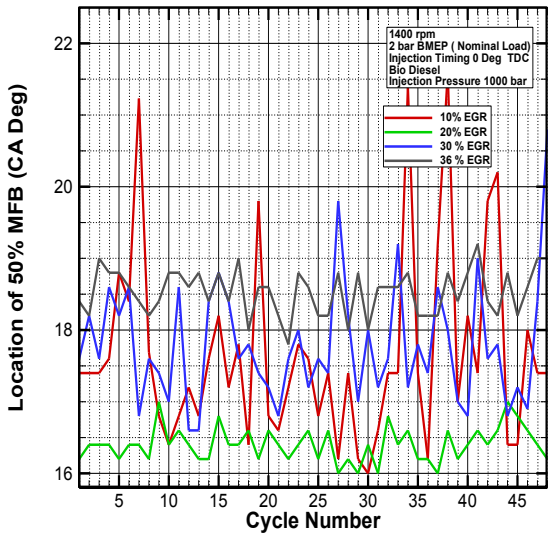

Figure 18: Location of 50% mass fraction burn versus cycle number for biodiesel

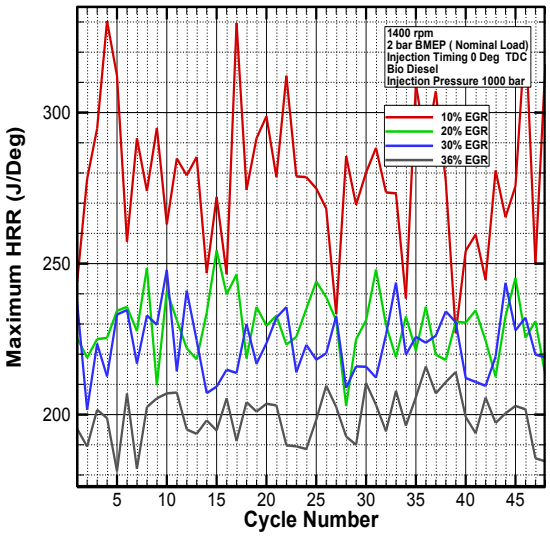

Figure 19: Maximum HRR versus cycle number for biodiesel

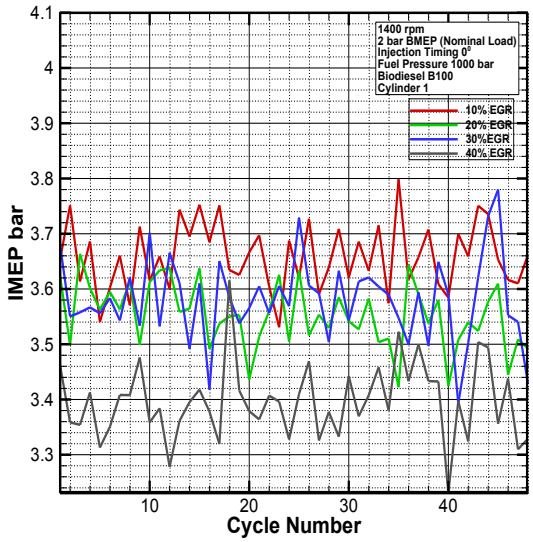

Figure 20: IMEP versus cycle number for biodiesel

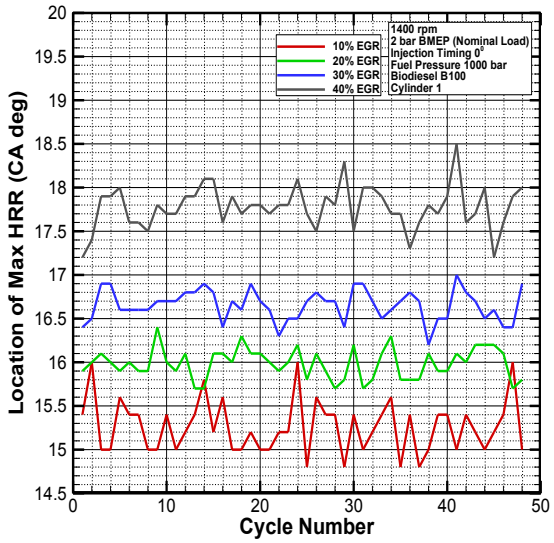

Figure 21: Location of maximum heat release rate versus cycle number for biodiesel

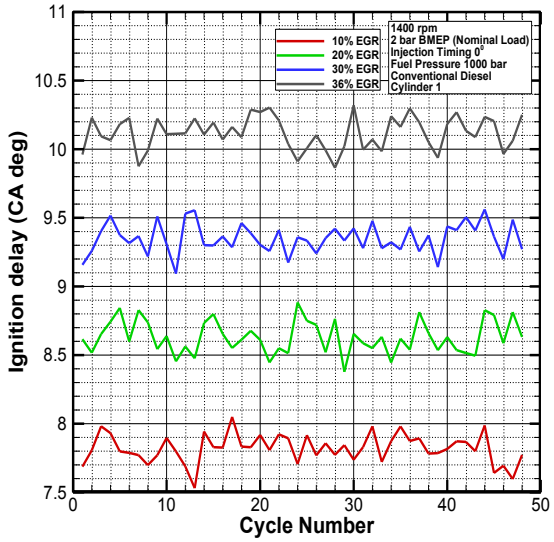

Figure 22: Ignition delay versus cycle number for biodiesel

Figure 12 to Figure 22 represents the cyclic variation of peak pressure, location of peak pressure, Maximum heat release rate and location of 50% Mass fraction burn respectively for biodiesel. The data represented are for cylinder 1, which is representative of the average for all four cylinders. Each combustion characteristic is analyzed for all EGR levels that where used in section 4.1. It is clear that based on visual confirmation there is no recurring pattern for 50 continuous cycles. The observed variation in the two sets of plots is occurring over a very small-scale of combustion phasing parameters. In addition, there is no predominant cycle that causes variation in subsequent cycles, which is clear from the minor variation in the magnitude and location of maximum heat release rate.

4.3 Effect of exhaust gas constituents

The objective of this section is to determine if the difference of exhaust gas species is the source for the difference of the cool flame characteristics between the two fuels. Exhaust gas consists of species that are completely reacted (carbon dioxide, water, nitrogen dioxide), constituents in their elemental states (predominantly oxygen and nitrogen) and constituents that have partially reacted (carbon monoxide and unburned hydrocarbon). The study is based on the assumption that trace elements present in the EGR have no effect on the subsequent combustion process. The completely reacted species form a filler material absorbing the heat released by the fuel reducing the overall in-cylinder temperature, while the some constituents in the elemental state acts as filler (nitrogen)

and others participate in the reaction (oxygen, nitrogen). The partially reacted constituents could undergo complete oxidation affecting the in-cylinder combustion process. The section is aimed at determining if difference in concentration of the partially burned species is the reason for the absence of the cool flame in biodiesel, operating in low temperature combustion mode.

Reaction 4 represented below describes the mechanism of oxidation of HC and CO. The hydrocarbon in the chemical equation represents the fuel. The oxygen insufficiency is due to the local equivalence ratio variation, because the diesel engines operate lean. The increase in local equivalence ratio is attributed to the EGR decreasing overall air intake. Reactions 5 and Reactions 6 represent exothermic oxidation of the partially burned EGR constituents, which is postulated to aid in smooth transition from the cool flame combustion to the high temperature combustion.

$$Hydrocarbon + \mathrm{I}nsufficient\ O_2 \rightarrow\ HC + CO + CO_2 + H_2O \quad \text{…..(9)}$$

$$HC + O_2 \rightarrow\ H_2O + CO_2 \quad \text{……..(10)}$$

$$CO + H_2O \rightarrow CO_2 + H_2 \quad \text{……(11)}$$

Figure 23 shows the variation of combustion efficiency with respect to EGR level for both biodiesel and conventional petroleum diesel. It is evident that the fuel conversion of biodiesel is lower in comparison to conventional petroleum diesel, suggestive of higher partially burned constituents in the exhaust of biodiesel.

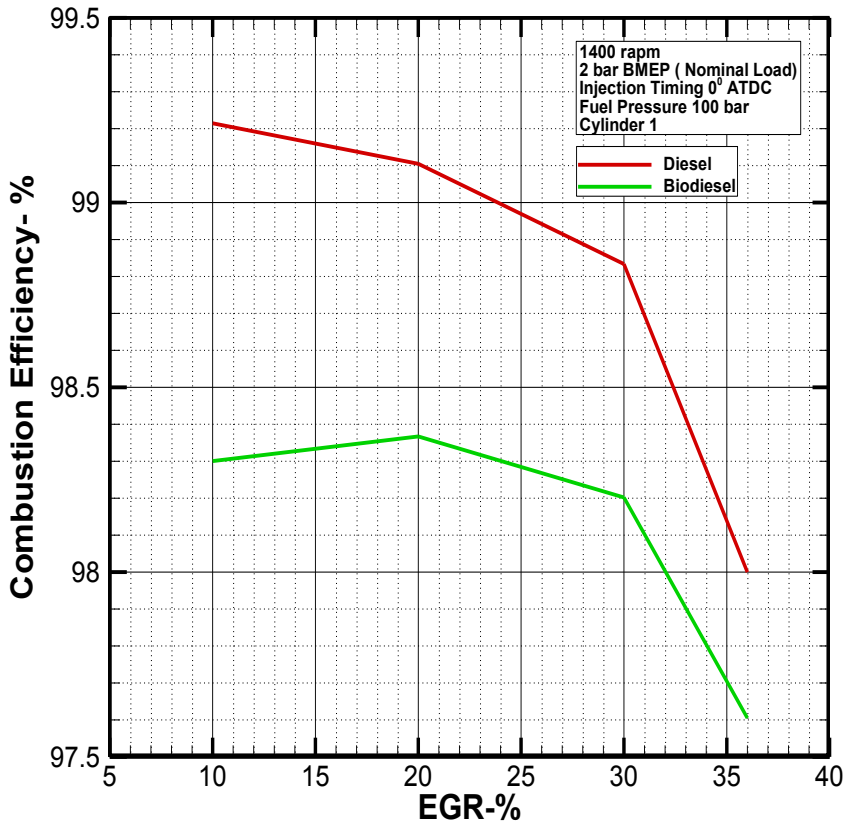

Figure 23: Combustion efficiency versus EGR level

Figure 24 represents the carbon monoxide and HC concentration of biodiesel and petroleum diesel, respectively. The trends are coherent to that of the combustion efficiency. The higher combustion efficiency of petroleum diesel results in lower CO and HC emissions in comparison to biodiesel.

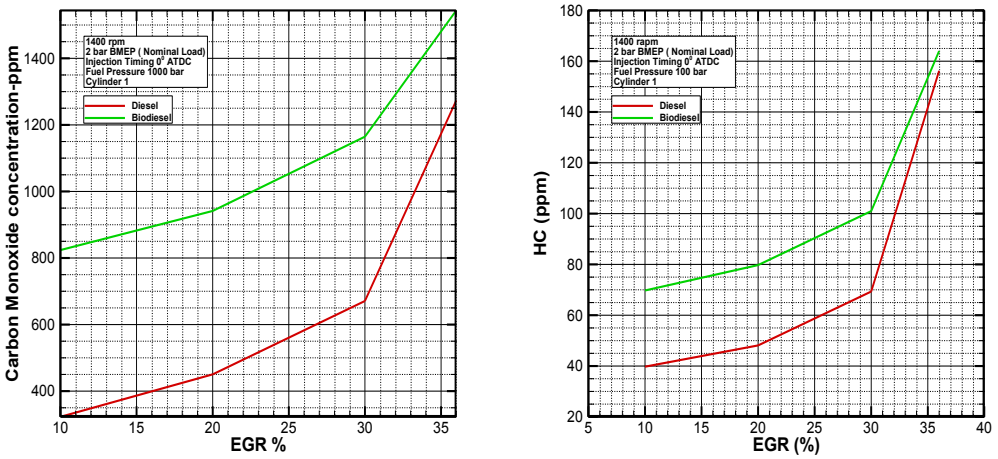

Figure 24: Variation of a) carbon monoxide Concentration b) unburned hydrocarbon as a function of EGR.

The optical visualization studies conducted by of Lyle et al. [30] shows the disappearance of the fuel spray during the cool flame combustion. Based on his observation and the difference in the exhaust gas species, there could be a possibility that the combustion of the partially combusted exhaust gas constituents could aid in the smooth transition from the low temperature cool flame combustion to the high temperature combustion for biodiesel. The possibility can be confirmed by comparing the heat released by the oxidation of the partially reacted exhaust gas components with the inflection zone between the low and high temperature heat release.

Table 7 contains the energy released by combustion of the individual and overall heat released by the complete combustion of partially burned exhaust gas species. The energy released for CO was calculated using the standard enthalpy of combustion ΔH_C obtained from literature [39]. With no knowledge of specific species composing the HC concentrations, a worst-case assumption of the heating value of CH_4 is made. The calorific value of methane was obtained from literature is used in the heat release calculation. The calculation of the heat released provided in Table 7 is included in the appendix.

Table 7: Energy released by combustion exhaust gas species for biodiesel

Energy Released by HC combustion (J)	Energy Released by CO combustion (J)	Total Energy Released (J)
0.0997	0.4191	0.4191
0.1018	0.4277	0.4277
0.1166	0.4815	0.4815
0.1628	0.6014	0.6014

The actual heat released by the combustion of the partially burned constituents will be lower than the total energy presented in Table 7 due to the fact that heating value of HC will be lower than the assumption and the assumption of complete combustion of the all partially reacted constituents between cool flame and high temperature combustion.

In addition to this shows the energy released by the complete combustion of the partially burned constituents in the EGR for petroleum diesel. The difference in energy released between the two fuels, compared to the total energy of the inflection zone after cool flame combustion in Figure 4 it is evident that the combustion of the partially burned exhaust gas constituents is unlikely responsible for the smooth transition from low temperature cool flame combustion to high temperature combustion in the case of biodiesel.

Table 8: Energy released by complete combustion of partially combusted products

Energy Released by HC combustion (J)	Energy Released by CO combustion (J)	Total Energy Released (J)
0.0583	0.1867	0.2450
0.0630	0.2229	0.2858
0.0830	0.3054	0.3883
0.1440	0.4798	0.6238

4.4 Effect of rail pressure

The objective of this section is to determine the effect of rail / injection pressure on the cool flame combustion characteristics of biodiesel. The rail pressure is varied at a constant EGR rate to determine if the there are changes in the combustion

characteristics. The EGR level is maintained at the maximum condition of 36% for better stabilization of the start of combustion. The study is based on the study conducted by Bittle et al. [40] on the effect of the fuel injection pressure on the cool flame for petroleum diesel; that study describes the shift phenomenon of the cool flame as injection pressure increases. The shift has been attributed to the fuel droplet size and the change in the in-cylinder mixing phenomenon. Figure 25 shows the apparent rate of heat release for petroleum diesel for various injection/rail pressures at maximum EGR condition. From the figure it is clear that the results of this study are concurrent with those of Bittle et al.[40]. This section is directed towards the determination of the existence of the cool flame upstream of the high temperature combustion, to rule out the dependency of cool flame on the chemical composition of the fuel.

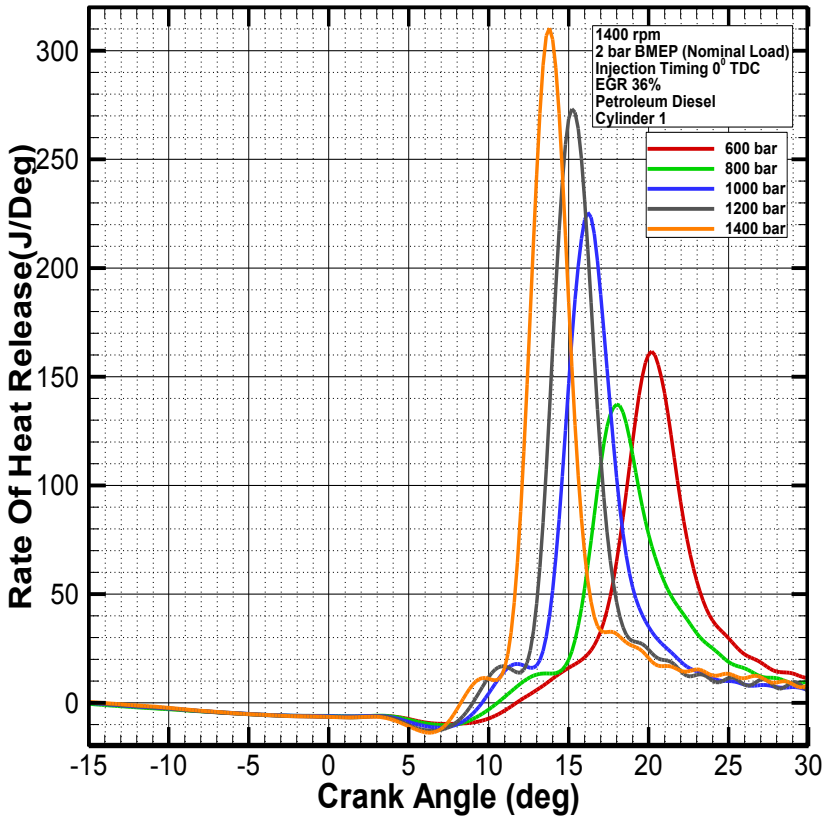

Figure 25: Rate of heat release versus crank angle as a function of rail pressure for petroleum diesel.

Figure 26 represents the effect of rail pressure on apparent rate of heat release of biodiesel at maximum EGR condition (36%). From the figure it can be seen that the cool flame like characteristic can be seen at rail pressures above 1000 bar. But it is still unclear that if the hump that is seen is the cool flame characteristic.

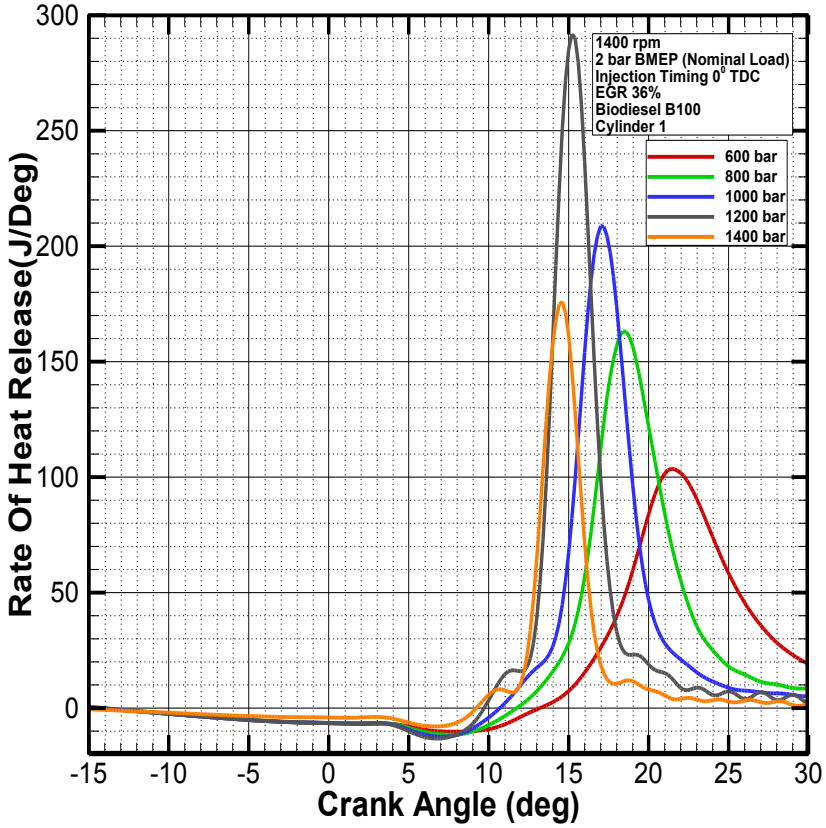

Figure 26: Rate of heat release versus crank angle as a function of rail pressure for biodiesel B100

Flame lift off is defined as the quasi-steady distance between the tip of the injector to the base of the flame kernel. In general flame lift off is defined during that of diffusion combustion, as the fuel injected burns continuously in contrast to that of premixed combustion. The "hump" that is observed in Figure 26 could be associated with premixed heat release observed with that of lifted flame combustion. Lifted flame combustion is a type of diffusion combustion with long lift off length; some premixed

heat release may occur during the lift-off length development as a diffusion reaction establishes in a lifted flame fashion. Lifted flame combustion is a type of diffusion combustion with long lift off length; some premixed heat release may occur during the lift-off length development as a diffusion reaction establishes in a lifted flame fashion. To understand if the hump seen in the Figure 25 and Figure 26 is cool flame it must be understood and the if the combustion process is strictly adhering to the low temperature combustion principle. In conventional flame combustion hydrocarbon molecules break down and react with oxygen producing carbon-di-oxide and water, but in the case of cool flame combustion the molecules break into larger fragments, which easily recombine, with each other. A quasi-steady equilibrium exists between the fragmentation and recombination of the fuel molecules resulting in the release of much less heat, light and carbon dioxide in comparison to conventional flame combustion. As described above, such behavior leads to NTC behavior during cool flame events.

Figure 27 shows the variation of rate of heat release and temperature with crank angle for a rail pressure of 1200 bar. It can be seen from the figure that temperature remains relatively constant during the first hump that is observed in the crank angle range of 10 to 13 degrees.

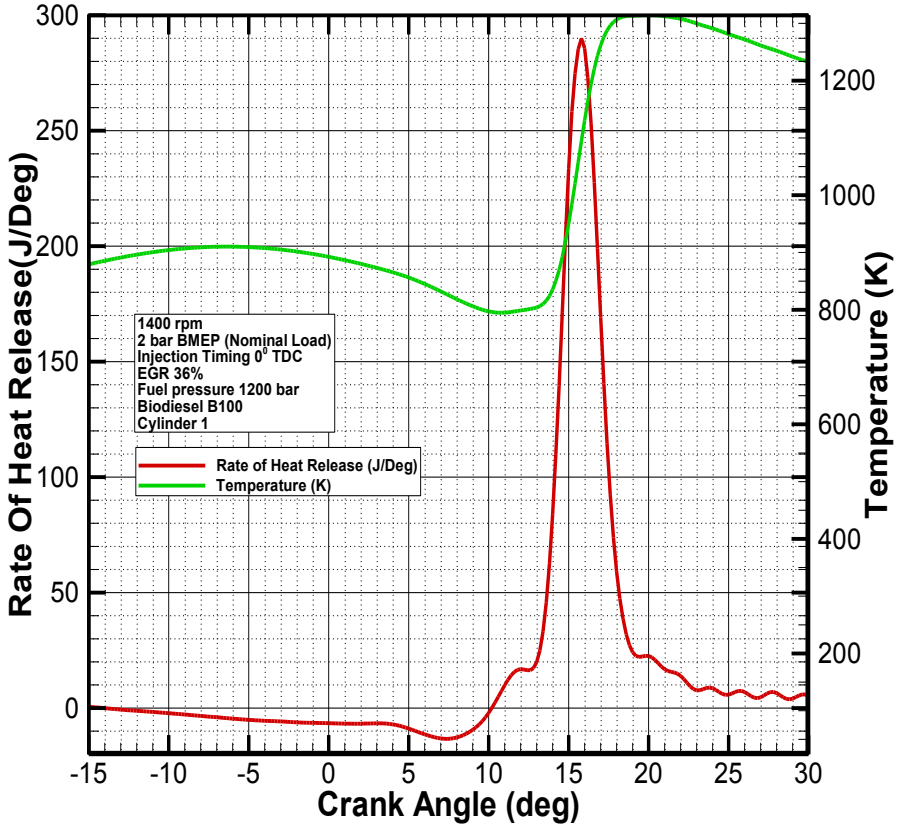

Figure 27: Rate of heat release and temperature versus crank angle for biodiesel at a rail pressure of 1200 bar

Figure 28 shows the variation of rate of heat release and temperature with respect to crank angle for a rail pressure of 1400 bar. From the figure it can be inferred that the temperature remains relatively constant during the first hump that is observed during the crank angle range of 8 to 12 degrees.

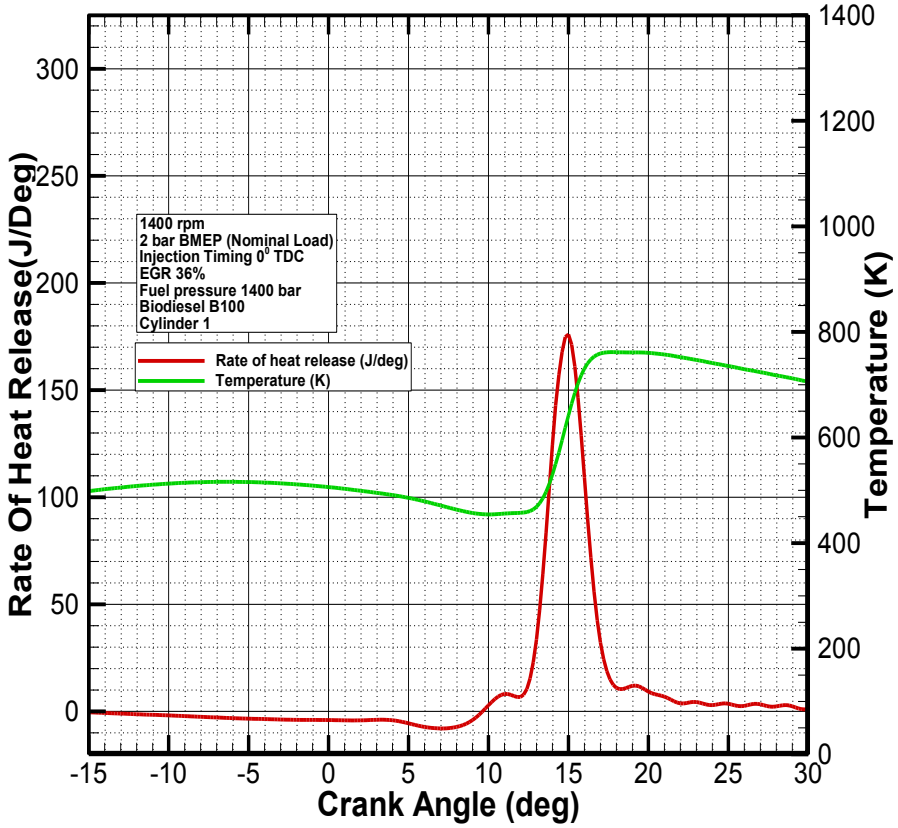

Figure 28: Rate of heat release and temperature versus crank angle for biodiesel at a rail pressure of 1400 bar

From the above discussion it is clear that the cool flame is present for higher rail pressure operation of rail pressure. In order to ensure that the combustion operation is still in LTC mode the phasing of the physical and chemical in-cylinder processes. The physical process includes the fuel injection, mixing and latent heat of vaporization of the fuel. The chemical process involves the oxidation reaction of the fuel releasing energy .In conventional combustion the physical and chemical processes occur together. During

the diffusion combustion phase of conventional combustion the fuel injection, air fuel mixing and combustion occurs simultaneously for parcels of fuel introduced at different times during the process. The vice versa occurs in low temperature combustion where the physical and chemical processes are spatially and temporarily separate making the combustion completely premixed. Taking the start of combustion as the 1% mass fraction burn, the following Table 9 shows the data for the crank angle location of the start of end of fuel injection and start of combustion for the higher rail pressure conditions exhibiting the cool flame behavior.

Table 9: Comparison of end of injection and the start of combustion for higher rail pressures for biodiesel operating in LTC combustion mode

Rail Pressure (bar)	End of Injection (CA Deg)	Start of Combustion (Ca Deg)
1200	6.9	12.09388
1400	6.5	10.72

From Table 9 it is clear that the physical and the chemical processes are separate for higher rail pressure of biodiesel despite the presence of cool flame.

As shown in Figure 26, this study observes cool flame behavior for the studied soy-based biodiesel. Tompkins, et al. [12], however, did not observe cool flame behavior for their studied palm-based biodiesel. Tompkins et al. [13] suggests that the presence of the cool is purely due to the difference in the chemical composition of the fuel, in particular the oxygen content of the fuel (biodiesel). To understand this discrepancy, a final consideration is given for the fuel penetration behavior between the fuels under LTC conditions.

4.5 Effect of fuel penetration and mixing

The objective of the section is to discuss the combined effect of fuel penetration, fuel air mixing and equivalence ratio on biodiesel cool flame combustion. The variation of each characteristic will be discussed separately and the combined effect will be summarized.

From the previous section it is clear that the partially burned exhaust gas constituents are not responsible for the smooth transition from low temperature cool flame combustion to high temperature combustion and that cool flame exists at higher injection/rail pressures for biodiesel. The fuel penetration length is calculated for each test point of the study using the correlations that are provided are provided Heywood [23], for both petroleum diesel and biodiesel. All studied conditions, including those that vary EGR level with constant rail pressure, are evaluated in terms of fuel penetration length.

Figure 29 and Figure 30 show the fuel penetration length as a function of EGR and rail pressure, respectively for both studied fuels (petroleum diesel and biodiesel). The calculation of the fuel penetration length is presented in the appendix section for each parameter sweep. From the figures it is evident that the fuel penetration length increases with both increase in EGR and rail pressure. The increase in fuel penetration length for the EGR sweep is caused by the decrease in the in-cylinder gas density with increase in EGR level and penetration length increases with increase in rail pressure due to the increased pressure difference between the cylinder contents and the fuel injection system. This is evident from the data presented in the appendix.

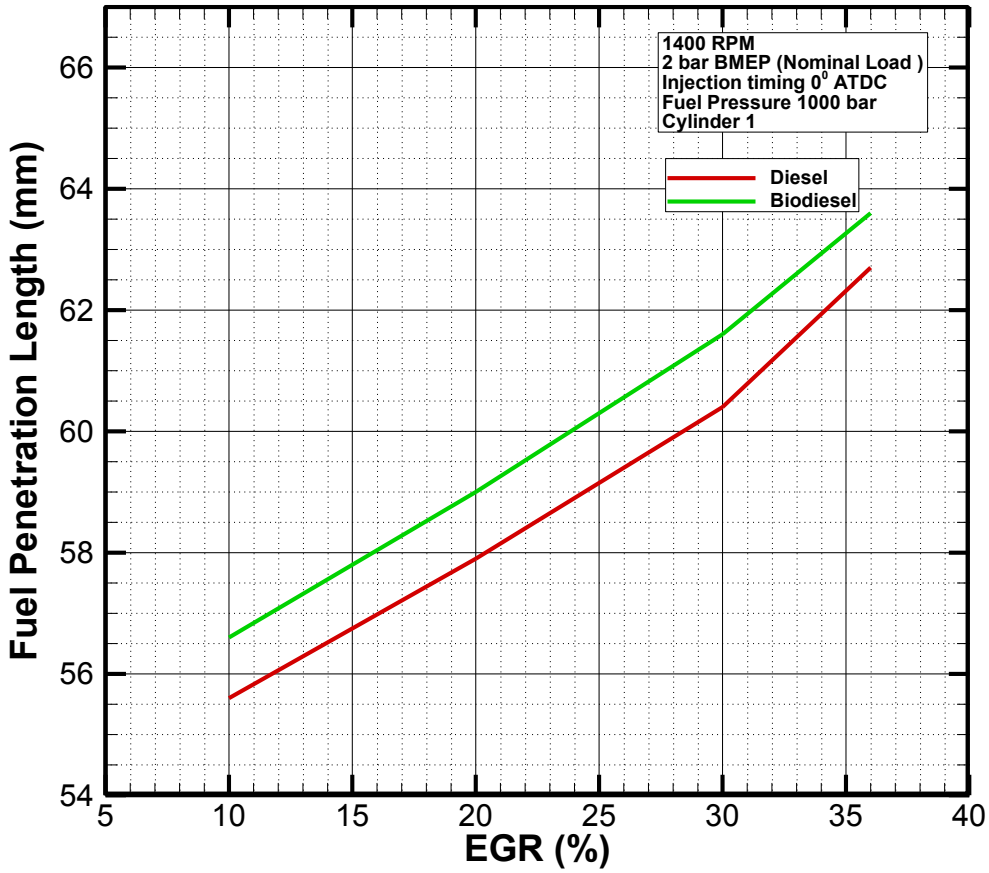

Figure 29: Fuel penetration length (mm) versus EGR level (%)

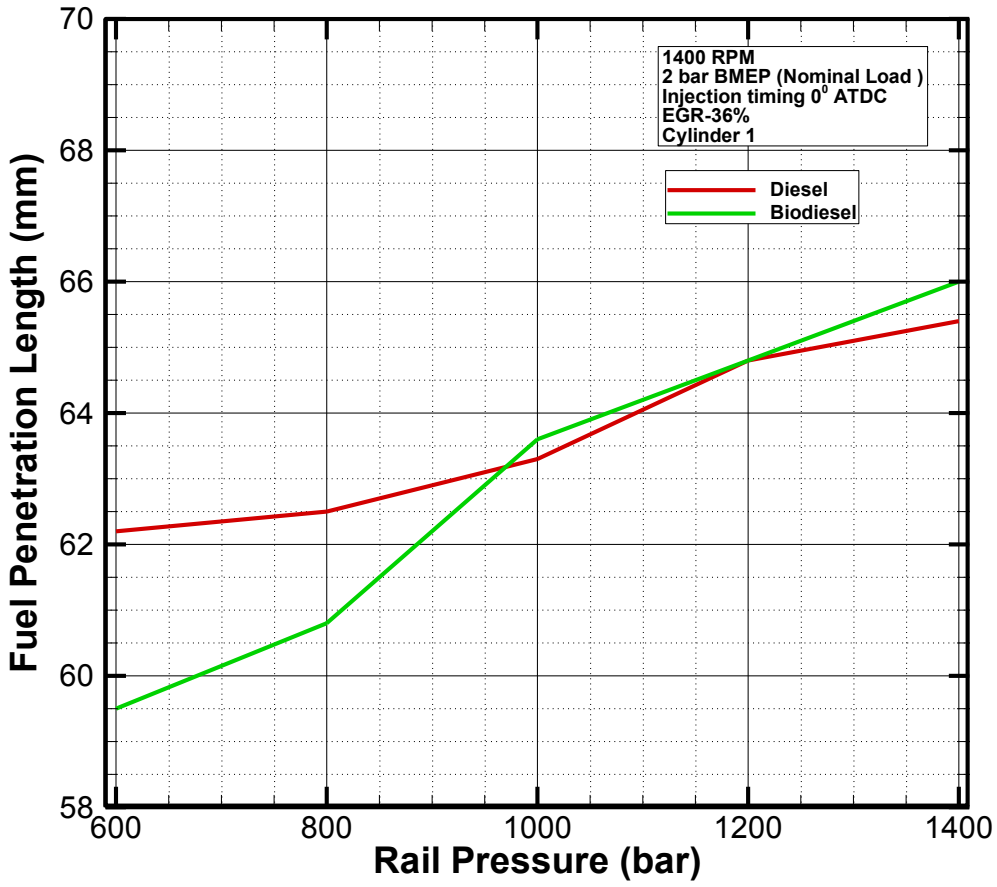

Figure 30: Fuel penetration length (mm) versus rail pressure (bar)

For both parameters, EGR and rail pressure the fuel penetration length increases with increase in the varied parameter. A particular aspect to be noted from Figure 29 and Figure 30 is that the fuel penetration length increase is greater with increase in rail pressure for both fuels in comparison to increase in EGR. In particular the fuel penetration length is greater for rail pressure values of 1200 bar, 1400 bar in Figure 30 compared to the 36% EGR condition in Figure 29.

The second characteristic considered in the study is the equivalence ratio. Since the EGR level is maintained constant for rail pressure sweep of both the fuels, the variation in the overall equivalence ratio should be minimal. Figure 31 shows the variation of overall equivalence ratio as a function of rail/injection pressure for both fuels, whose trend ascertains the above. The other equivalence ratio that is used later in the discussion is the local equivalence ratio, which has no direct means of measurement within the study's capability.

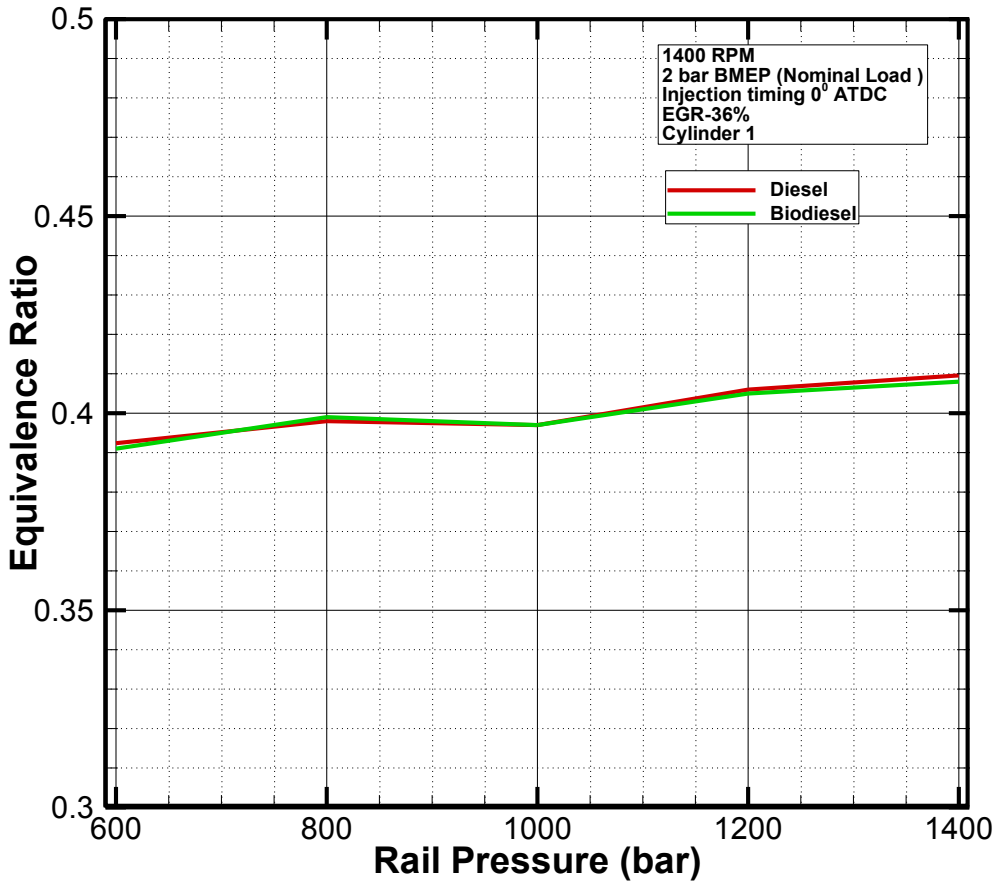

Figure 31: Equivalence ratio versus rail pressure (bar)

Cool flame combustion mechanism is observed for almost all combustion processes, even when their combustion phasing is coincident with that of high temperature heat release making it unobservable in heat release profiles. This is demonstrated by optical studies conducted by Lyle et al. [41] by blanking the high temperature heat release using filters, revealing the existence of cool flame during the high temperature combustion. In the case of the rail pressure sweep of biodiesel a spatial shift of the cool flame occurs with increase in rail pressure beyond 1000 bar making the cool flame visible in the heat release profile, whose cause can be postulated based on the combined effect of the fuel penetration length and equivalence ratio. The work of Fish et al. [20] has demonstrated the dependency of the cool flame on the equivalence ratio. The major change observed with increase in fuel penetration length and fairly constant equivalence ratio is change in the local equivalence ratio, especially near the fuel injector where the cool flame has been observed in optical studies [30,41,42].

The increase in fuel penetration length decreases the local equivalence ratio near the fuel injector, thereby decreasing the time required to form the combustible mixture (ignition delay), which can be seen by overall shift in the heat release profile with increase in rail pressure in Figure 26. With the increase in fuel penetration length the equivalence ratio near the fuel injector decreases to a point to support cool flame combustion and not high temperature combustion. This is supported by the studies conducted by Lyle et al. [30] , which shows the complete disappearance of the fuel spray during the cool flame combustion duration. Conversely at lower fuel penetration lengths, the time required for

the mixing should be same for both cool flame and high temperature combustion making the cool flame unobservable in the heat release profile.

Based on the above discussion of the effect of local equivalence ratio on the cool flame combustion characteristic, the oxygen content of the biodiesel should aid in lowering the local equivalence ratio and making the cool flame observable at lower rail pressures in comparison to petroleum diesel. This is not the case in this study, due to the longer injection of biodiesel in comparison to petroleum diesel, due to the lower fuel heating value of biodiesel.

The optical studies of Lyle et al. [30] show the shift in the spatial location of the cool flame based on the ambient oxygen concentration, in particular the upstream formation of the cool flame with decrease in ambient oxygen concentration. Extending the effect to the EGR sweep on both the fuels, the increase in EGR causes the decreases in ambient oxygen concentration. The decrease in ambient oxygen concentration is sufficient to cause an upstream shift of the cool flame for all EGR condition as seen in Figure 3 and the oxygen content of the biodiesel prevents the upstream shift of the cool flame. Tompkins et al. [13] observed this in his study of the effect of oxygenated fuels on low temperature combustion.

V. CONCLUSIONS

The objective of the study has been satisfied by successful analysis of the difference in the cool flame characteristics between soybean biodiesel and conventional petroleum diesel. A summary of the major findings of this study is

- The observed cool flame is not an outcome of systemic error caused by variations of successive cycles of operation or the difference in the partially combusted products in the re-circulated exhaust gas.
- The cool flame is not solely a property of the fuel as it exists in all combustion processes and is mostly at the same spatial location of the high temperature heat release making it unobservable in most heat release profiles.
- Cool flame exists for biodiesel at higher rail pressure in comparison petroleum diesel (where it exists at most operating conditions of LTC).
- The increase in rail pressure of biodiesel causes a decrease in the local equivalence ratio to a point to support only cool flame combustion (disappearance of vapor spray and NTC). This is seamlessly followed by injection, mixing and simultaneous latent heat absorption of fuel from the surroundings causing an inflection point between low temperature cool flame and high temperature heat release.

In conclusion, this study shows using its own data and findings described in literature that biodiesel may exhibit cool flame behavior in heat release profiles of low temperature combustion, depending on the fuel's oxygen content, cetane number, and in-cylinder conditions during injection and ignition events. Although not fully vetted in this study, such appearance of cool flame behavior with biodiesel low temperature combustion can have effects on low temperature combustion efficiency and emissions, as described in literature.

REFERENCES

[1] US EPA C. C. D., “Carbon di-oxide” [Online]. Available: http://www.epa.gov/climatechange/ghgemissions/gases/co2.html. [Accessed: 14-Jan-2014].

[2] U.S, EIA, “Effects of green house gases other than carbon di-oxide” [Online]. Available: http://www.eia.gov/todayinenergy/detail.cfm?id=1390. [Accessed: 20-Sep-2013].

[3] U.S, EPA U., “Nitrogen di-oxide (NO2)” [Online]. Available: http://www.epa.gov/airtrends/aqtrnd95/no2.html. [Accessed: 06-Sep-2013].

[4] US EPA R. 7, “Air quality programs” [Online]. Available: http://www.epa.gov/region07/air/quality/pmhealth.htm. [Accessed: 17-Sep-2013].

[5] EUR-Lex, “Recherche simple” [Online]. Available: http://eur-lex.europa.eu/LexUriServ/LexUriServ.do?uri=CELEX:31998L0069:EN:NOT. [Accessed: 14-Jan-2014].

[6] European Union legislation, “EURO emission standard” [Online]. Available: http://europa.eu/legislation_summaries/environment/air_pollution/l28186_en.html. [Accessed: 20-Sep-2013].

[7] EPA U., “Federal emission standard” [Online]. Available: http://www.epa.gov/otaq/standards/allstandards.htm. [Accessed: 20-Sep-2013].

[8] European Union, “EURO standard” [Online]. Available: http://www.ngk.de/en/technology-in-detail/lambda-sensors/basic-exhaust-principles/euro-standards/. [Accessed: 20-Sep-2013].

[9] Gomaa, Aimin, Kamarudin, 2010, "Trade-off between NOx, soot and EGR rates for IDI diesel engine fuelled with JB5," World Academy of Science, Engineering and Technology, Connecticut, USA.

[10] Tanabe K., Kohketsu S., and Nakayama S., 2005, Effect of Fuel Injection Rate Control on Reduction of Emissions and Fuel Consumption in a Heavy Duty DI Diesel Engine, SAE International, Warrendale, PA.

[11] Mendez S., Kashdan J. T., Bruneaux G., Thirouard B., and Vangraefschepe F., 2009, Formation of Unburned Hydrocarbons in Low Temperature Diesel Combustion, SAE International, Warrendale, PA.

[12] Brijesh P., Chowdhury A., and Sreedhara S., 2013, Effect of Ultra-Cooled EGR and Retarded Injection Timing on Low Temperature Combustion in CI Engines, SAE International, Warrendale, PA.

[13] Tompkins B. T., and Jacobs T. J., 2012, "Low temperature combustion with biodiesel: The role of oxygenation in improving efficiency and emissions," Spring Tech. Meet. Cent. Sect. Combust. Inst., **2**.

[14] Lindström B., Karlsson J. A. J., Ekdunge P., De Verdier L., Häggendal B., Dawody J., Nilsson M., and Pettersson L. J., 2009, "Diesel fuel reformer for automotive fuel cell applications," Int. J. Hydrog. Energy, **34**(8), pp. 3367–3381.

[15] J. A. Barnard A. W., 1969, "Cool-flame oxidation of ketones," Symp. Int. Combust., **12**(1), pp. 365–373.

[16] Center A. R., 1999, Research & Technology, DIANE Publishing, UK.

[17] Fredholm O., Jacobsson A., and Pasman H. J., 2001, Loss Prevention and Safety Promotion in the Process Industries, Elsevier, Amsterdam.

[18] Scott S. K., 1993, Chemical Chaos, Oxford University Press, Oxford, England.

[19] Gray P., and Scott S. K., 1994, Chemical Oscillations and Instabilities: Non-linear Chemical Kinetics, Clarendon Press, UK.

[20] Fish A., 1968, "The cool flames of hydrocarbons," Angew. Chem. Int. Ed. Engl., **7**(1), pp. 45–60.

[21] Pease R. N., 1929, "Characteristics of the non-explosive oxidation of propane and the butanes1," J. Am. Chem. Soc., **51**(6), pp. 1839–1856.

[22] US EPA E. R. C., "Improved method of heating catalytic converters of vehicles to attain ultra-low emissions" [Online]. Available: http://cfpub.epa.gov/ncer_abstracts/index.cfm/fuseaction/display.abstractDetail/abstract/1535. [Accessed: 18-Sep-2013].

[23] Heywood J. B., 1988, Internal Combustion Engine Fundamentals, McGraw-Hill, New York.

[24] Finol Parra C., 2008, "Heat transfer investigation in a modern diesel engine", Masters thesis, University of Bath, UK.

[25] Dent J. C., 1971, A Basis for the Comparison of Various Experimental Methods for Studying Spray Penetration, SAE International, Warrendale, PA.

[26] Kumar A. P., Annamalai K., and Premkartikkumar S. R., 2013, "Influence of injection timing on emission parameters of adelfa biodiesel (nerium oil methyl ester–nome) fuelled diesel compression ignition engine," IJITR, **1**(1), pp. 099–102.

[27] Murugesan A., Subramaniam D., Avinash A., and Nedunchezhian N., 2013, "A comprehensive view on performance, emission, and combustion characteristics of biodiesel-diesel blends at advanced injection timings," J. Renew. Sustain. Energy, **5**(3), pp. 033103–033103–10.

[28] Bittle J. A., Knight B. M., and Jacobs T. J., 2009, The Impact of Biodiesel on Injection Timing and Pulsewidth in a Common-Rail Medium-Duty Diesel Engine, SAE International, Warrendale, PA.

[29] Zhang J., and Fang T., 2011, Spray Combustion of Biodiesel and Diesel in a Constant Volume Combustion Chamber, SAE International, Warrendale, PA.

[30] Pickett L. M., Kook S., and Williams T. C., 2009, Visualization of Diesel Spray Penetration, Cool-Flame, Ignition, High-Temperature Combustion, and Soot Formation Using High-Speed Imaging, SAE International, Warrendale, PA.

[31] Knight B. M., Bittle J. A., and Jacobs T. J., 2010, "Efficiency considerations of later-phased low temperature diesel combustion," ASME 2010 Intern. Combust. Engine Div. Fall Tech. Conf., pp. 359–368.

[32] Moriyoshi Y., Kamimoto T., and Yagita M., 1993, Prediction of Cycle-to-Cycle Variation of In-Cylinder Flow in a Motored Engine, SAE International, Warrendale, PA.

[33] Zheng M., and Reader G. T., 1995, "Preliminary investigation of cycle-to-cycle variations in a nonair-breathing diesel engine," J. Energy Resour. Technol., **117**(1), pp. 24–28.

[34] Maurya R. K., and Agarwal A. K., 2009, Experimental Investigation of Cycle-by-Cycle Variations in CAI/HCCI Combustion of Gasoline and Methanol Fuelled Engine, SAE International, Warrendale, PA.

[35] Lu J.-H., and Lee Y.-B., 1996, Analysis and Measurements of Cyclic Variations and Emissions of Single Cylinder Two Stroke Engines at Low Loads, SAE International, Warrendale, PA.

[36] Samuel S., Morrey D., Whelan I., and Hassaneen A., 2010, Combustion Characteristics and Cycle-By-Cycle Variation in a Turbocharged-Intercooled Gasoline Direct-Injected Engine, SAE International, Warrendale, PA.

[37] Sztenderowicz M. L., and Heywood J. B., 1990, Cycle-to-Cycle IMEP Fluctuations in a Stoichiometrically-Fueled S.I. Engine at Low Speed and Load, SAE International, Warrendale, PA.

[38] Dai W., Trigui N., and Lu Y., 2000, Modeling of Cyclic Variations in Spark-Ignition Engines, SAE International, Warrendale, PA.

[39] Wikipedia, "Carbon Monoxide" [Online]. Available: http://en.wikipedia.org/w/index.php?title=Carbon_monoxide&oldid=571226673. [Accessed: 04-Sep-2013].

[40] Bittle J. A., and Jacobs T. J., 2012, "On the relationship between fuel injection pressure and two-stage ignition behavior of low temperature diesel combustion," J. Energy Resour. Technol., **134**(4), pp. 042201–042201.

[41] Pickett L. M., Siebers D. L., and Idicheria C. A., 2005, Relationship Between Ignition Processes and the Lift-Off Length of Diesel Fuel Jets, SAE International, Warrendale, PA.

[42] Yamada H., Goto Y., and Tezaki A., 2006, Analysis of Reaction Mechanisms Controlling Cool and Thermal Flame with DME Fueled HCCI Engines, SAE International, Warrendale, PA.

APPENDIX A: FUEL PENETRATION CALCULATION

Test point

Fuel: Petroleum diesel

Fuel injection pressure: 1000 bar

EGR level: 10%

Engine speed: 1400 rpm (23.34 rps)

Nominal Load: 2 bar BMEP

Calculation

Duration for one crank angle rotation= $\frac{1}{360\times1400} = 0.000119048$ s/Deg

Time duration for air intake= $180\times0.0.000119048 = 0.00214$ s

Air flow rate = 61.04666 g/s

Mass of air flow = 61.0466 g/s x 0.00214 s = 0.001308143 kg

Fuel injection duration= 5.5474 Deg

Fuel injection time = 5.5474 Deg x 0.000119048 s/Deg = 0.660406548 ms

Fuel flow rate = 1.15472 g/s

Mass of fuel injected = 1.15472 g/s x 0.660406548 = 7.62585E-07 kg

Total mass in cylinder = mass of cylinder + mass of fuel = 0.001308905 kg

Volume of cylinder = 0.000078 m^3

Density of cylinder = 0.001308 kg/ 0.000078 m^3 = 16.78083717 Kg/m^3

In-cylinder pressure at the start of injection = 47.46074 bar

Pressure difference between the cylinder and fuel injection system $= 1000 - 47.46074$

$= 952.539260$ bar

Nozzle diameter = 0.00018 m

Temperature of gas = 877.7363 K

$$S = 3.07\left(\frac{952.54\times10^{5}}{16.78}\right)^{0.25}(0.0006604 \times 0.00018)^{1/2}\left(\frac{294}{877.7363}\right)^{1/4}$$

$$= 39.30 \text{ mm}$$

APPENDIX B: SAMPLE CALCULATION OF HEAT RELEASE FROM PARTIALLY BURNED EXHAUST GAS CONSTITUENTS

Test Point

Fuel: Biodiesel diesel

Fuel injection pressure: 1000 bar

EGR level: 10%

Engine speed: 1400 rpm (23.34 rps)

Nominal Load: 2 bar BMEP

Calculation

Concentration of HC = 69.74291 ppm

Concentration of CO = 823.7834 ppm

Duration for one crank angle rotation= $\frac{1}{360\times1400} = 0.000119048$ s/Deg

Time duration for air intake= $180\times0.0.000119048 = 0.00214$ s

Air flow rate = 61.04666 g/s

Mass of air flow = 61.0466 g/s x 0.00214 s = 0.001308143 kg

Fuel injection duration= 5.5474 deg

Fuel injection time = 5.5474 deg x 0.000119048 s/deg = 0.660406548 ms

Fuel flow rate = 1.15472 g/s

Mass of fuel injected = 1.15472 g/s x 0.660406548 = 7.62585E-07 kg

Total mass in cylinder = mass of cylinder + mass of fuel = 0.001308905 kg = 1.308905g

Mass of HC in exhaust = $69.74291 \times 1.308905 \times 10^{-6} = 9.9027 \times 10^{-5}$g

Mass of CO in the exhaust = $823.7834 \times 1.308905 \times 10^{-6} = 0.00107401$ g

Energy released by combustion of HC = 37.3 MJ/Kg

Energy released by combustion of CO = 10.12 MJ/Kg

Mass of HC recirculated = $9.9027 \times 10^{-6} \times 0.10 = 9.9027 \times 10^{-6}$ g

Mass of CO recirculated= $0.00107401 \times 0.10 = 0.000107401$ g

Energy released by combustion of HC = $9.9027 \times 10^{-6} \times 37.3 \times 10^{-6} = 0.33961$ J

Energy released by combustion of CO = $0.000107401 \times 10.12 \times 10^{-6} = 1.426214$ J

Total energy released = 0.339610 + 1.426214 = 1.77 J